



저작자표시-비영리-변경금지 2.0 대한민국

이용자는 아래의 조건을 따르는 경우에 한하여 자유롭게

- 이 저작물을 복제, 배포, 전송, 전시, 공연 및 방송할 수 있습니다.

다음과 같은 조건을 따라야 합니다:



저작자표시. 귀하는 원저작자를 표시하여야 합니다.



비영리. 귀하는 이 저작물을 영리 목적으로 이용할 수 없습니다.



변경금지. 귀하는 이 저작물을 개작, 변형 또는 가공할 수 없습니다.

- 귀하는, 이 저작물의 재이용이나 배포의 경우, 이 저작물에 적용된 이용허락조건을 명확하게 나타내어야 합니다.
- 저작권자로부터 별도의 허가를 받으면 이러한 조건들은 적용되지 않습니다.

저작권법에 따른 이용자의 권리는 위의 내용에 의하여 영향을 받지 않습니다.

이것은 [이용허락규약\(Legal Code\)](#)을 이해하기 쉽게 요약한 것입니다.

[Disclaimer](#)

工學碩士 學位論文

Indium-Tin-Oxide 인쇄박막 제작과 위험유해물질
센서 응용에 관한 연구

**Fabrication of layers based on printed Indium-Tin-Oxide
and their application to Hazard and Noxious Substance sensor**



韓國海洋大學校 海洋科學技術專門大學院

海洋科學技術融合學科

李錫煥

본 논문을 이석환의 공학석사 학위논문으로 인준함.



위원장 김준영 (인)

위원 장지호 (인)

위원 이문진 (인)

2016년 8월 24일

한국해양대학교 해양과학기술전문대학원

Contents

List of Tables	iv
List of Figures	v
Abstract	vii
1. Introduction	
1.1 Sensor technology	1
1.2 Sensor technology application	3
1.2.1 Necessity of Hazardous and Noxious Substances sensor	3
1.2.2 Current state of HNS sensing technology	4
1.3 Metal oxide based sensor	5
1.4 Properties of ITO (Indium Tin Oxide)	7
1.5 Proposal and purpose of this study	14
Reference	15
2. Experimental methods	
2.1 Film printing method	18
2.2 ITO layer printing	21
2.3 Characterization Methods	23
2.3.1 Optimization of ITO layer	23
2.3.2 Surface and material properties of printed layers	27
2.3.3 Sensor performances	39
Reference	41
3. Characteristics of ITO film by printing coat method	
3.1 Material properties of the ITO	43
3.2 Optimization of the printed ITO layer manufacturing method	45
3.2.1 Determination of printing patterns	45
3.2.2 Transfer ratio of the ITO layer	48
3.3 Properties of the printed ITO layer	50
3.3.1 Shape control	50
3.3.2 Electrical properties	52

3.3.3 Optical properties	54
3.4 Conclusion	56
Reference	57
4. HNS sensor based on printed ITO layer	
4.1 Introduction	59
4.2 Experiment details	60
4.3 Sensor properties	61
4.4 Sensor mechanisms	63
4.5 Conclusion	65
Reference	66
5. Characteristic evaluation of ITO sensor	
5.1 Introduction	67
5.2 Experiment details	67
5.3 Reliability of the sensor	68
5.3.1 Dynamic characteristics of ITO sensor	68
5.3.2 Robustness tests of ITO sensor	70
5.3.3 Selectivity of ITO sensor	73
5.4 Conclusion	75
Reference	76
6. Conclusion	77
Resume	78
Acknowledgement	80

List of Tables

Table 1.1 Summary on characteristic of metal oxide sensor	6
Table 1.2 Sensor properties of ITO compared by structure	13
Table 3.1 Optical microscope image of printed ITO layer	47
Table 3.2 Hall measurement of printed ITO layer and sputtered ITO layer	53



List of Figures

Fig. 1.1 The type of sensor that has been developed and studied.	2
Fig. 1.2 Crystal structure of ITO	9
Fig. 2.1 Schematic diagram of screen-printing process	20
Fig. 2.2 Summary of the screen printing process and experimental apparatus	22
Fig. 2.3 An illustration of the sessile drop technique	24
Fig. 2.4 Schematic diagram of optical microscope	26
Fig. 2.5 Schematic of diagram of SEM	28
Fig. 2.6 Schematic diagram of TEM	30
Fig. 2.7 Schematic of X-ray diffraction	32
Fig. 2.8 Bragg's law	32
Fig. 2.9 Recombination process of Photoluminescence spectra	34
Fig. 2.10 Schematic diagram of Photoluminescence	34
Fig. 2.11 Current-voltage measurement	36
Fig. 2.12 Characteristic of current-voltage	36
Fig. 2.13 Description of 4 - probe measurement	38
Fig. 2.14 Schematic diagram of ITO layer sensor measurement	40
Fig. 3.1 (a) Particle size distribution of ITO composites (the insert is the TEM image of it), (b) XRD pattern of ITO composite	44
Fig. 3.2 Effect of surface tension of paste on screen printability (a) separating (b) leveling	47
Fig. 3.3 The pattern shape dependence of paste ratio in screen printing. (a) Resistance of ITO printed films with various ITO:binder mixing ratio, and the reproducibility of ITO paste with various ITO:binder mixing ratio, (b) 1:1 ratio ($R_p = 98\sim 100\%$), (c) 1:2 ratio ($R_p = 100\sim 101\%$), (c) 2:1 ratio ($R_p = 73\sim 76\%$)	49
Fig. 3.4 (a) FE-SEM images of ITO layer (the inset is the cross section of it), (b) Photograph of the printed ITO layer sensor	51
Fig. 3.5 I-V characteristics of printed ITO layer and sputtered ITO films	53
Fig. 3.6 PL spectra of printed ITO layer	55
Fig. 4.1 Time resolved resistance change of the ITO layers soaked in the various solutions	62
Fig. 4.2 Mechanism of reducer agent for ITO layer	64
Fig. 4.3 Schematic of Electrical Double Layer	64

List of Figures

Fig. 5.1 Responses of the ITO sensor in (a) different NH_3 concentration, and (b) different temperature	69
Fig. 5.2 FE-SEM images of (a) as-printed ITO layer, (b) tested ITO layer, (c) as-printed ZnO layer, and (d) tested ZnO layer. The insets for each picture are corresponding XRD results	71
Fig. 5.3 (a) The aging test result of the ITO layer for 7 days at room temperature, (b) SEM image of ITO surface during the test	72
Fig. 5.4 Sensitivity change of the ITO layers soaked in the various pH liquids	74



국문 요약

Lee, Seok Hwan

Department of Ocean Science and Technology (OST) School, Korea Maritime
and Ocean University

센서는 대상물의 물리 또는 화학적 신호를 전기적인 신호로 대신하거나, 변형시키는 소자이며, 센서기술은 기계장치에 감각기능을 부여하는 기술로 인간의 감각기능을 확장하는 기술이다. 이러한 정보는 현재의 정보통신 기술과 맞물려 유용하게 사용되고 있다.

센서기술은 집적화, 지능화, 시스템화, 소형화 등의 경향이 나타나고 있다. 또한 가정에서부터 산업현장, 해양 및 우주탐사에 이르기 까지 광범위하게 활용되고 있다.

하지만 센서의 보다 폭넓은 활용을 위해서 개선되어야 할 점도 다수 존재한다. 센서의 응용의 관점에서는 집적화, 저전력, 친환경적인 센서의 중요성이 더해가는 상황이다. 이를 위해서는 센서의 신뢰성을 확보하고, 센서의 사용 환경에 알맞은 물질을 활용하는 새로운 기술의 도입이 요구된다.

본 연구에서는 위험유해물질 집적센서의 개발을 위하여 안정된 센서 재료의 선택과 경제적인 제작방법의 검토, 이를 통한 센서 제작 및 성능의 검증에 관하여 연구하였다.

우선 화학적으로 안정적인 금속 산화물 중 나노 입자를 활용하여 접촉면적을 넓힘으로써 높은 감도와 안정성을 확보할 수 있다고 판단하였다. 또한 금속 산화물 나노 입자를 이용하여 센서를 제작하기 위하여 인쇄공학적 접근법을 제안하였다. 이를 통하여 제작된 센서의 감지 성능과 사용할 환경에 대한 내구성 및 신뢰성에 대하여 검토하여 특수한 환경에서 신호를 검출할 수 있는 센서를 구현하였다.

특히 해양플랜트에서 활용될 수 있는 위험유해물질 센서를 구현할 목적으로 별도의 히터작동 없이 상온에서 폭발성 물질을 검출할 수 있는 기능을 구현하기 위한 감도의 향상과 해양이라는 특수한 환경에서의 신뢰성 있는 신호를 발생시키고 유지하기 위한 방법을 연구하였다.

제1장은 센서기술에 대한 기본적인 내용과 ITO의 물성, 그리고 위험유해물질 센서의 중요성 및 본 연구의 목적에 대하여 설명하였다.

제2장에서는 실험방법 부분으로서, 인쇄공학기술 및 인쇄공학기술을 이용한 ITO박막제작 방법에 대해 서술하고, 본 연구에 사용된 특성 분석 기술에 대해 설명하였다.

제3장에서는 인쇄공학기술로 제작된 ITO 센서의 특성을 개선시키기 위한 최적화에 대하여 고찰하였고, 이를 적용한 인쇄된 ITO 박막의 물성평가 결과에 대해 설명하였다.

제4장에서는 제작된 ITO의 실온에서의 위험유해물질에 대한 센서 성능과 응용에 관하여 고찰하였다.

제5장에서는 제작된 ITO의 신뢰성 및 특성 변화 와 그 원인에 대한 고찰 결과를 설명하였다.

마지막으로 제6장에서는 본 연구에서 얻은 결과를 정리하여 요약 및 결론에 대하여 기술하여, 본 연구에서 목적인 안정성이 높은 위험유해물질 센서를 구현하였으며, 경제적인 방법으로 센서를 제작할 수 있음과, 이러한 센서를 통하여 신뢰성 있는 신호를 발생할 수 있음을 입증하였다.

KEY WORDS: Sensor, Indium tin oxide (ITO), hazardous and noxious substances (HNS), Marine pollution, Environmental monitoring

Abstract

Lee, Seok Hwan

Department of Ocean Science and Technology (OST) School, Korea Maritime
and Ocean University

A sensor is a device that converts physical or chemical states of a matter into an electrical signal. Sensor technology can be described as a technology that expands a human sense to a machine. And those information are used valuably in accord with present IT technology.

Sensor technology clearly reveals a tendency of miniaturization, integration, intellectualization, and systematization etc. Furthermore, it has been used extensively from our daily life to marine or space exploration.

However, At the field of application, sensor technology should be improved in many aspects. Moreover, I felt the need to develop environmentally friendly and Low-power sensor is growing. Also, Introduction of new technology is required to take of suitable material in harsh environments. And reliability is inevitable.

In this thesis, I have researched a new hazardous and noxious substances sensor to apply for offshore plants and seacoast.

I considered that higher sensitivity and stability could be acquired by using chemically stable metal oxides. Especially, metal oxide nano particles will be suitable since it provides wide contact surface. In addition, I suggested a print coating technology to fabricate the sensors. Using this method, I have demonstrated the hazardous and noxious substances sensor, and verified the feasibility of the sensors at harsh environments.

In the chapter 1, I described the sensor technology, physical properties of ITO, the importance of hazardous and noxious substances sensor, and the purpose of this dissertation.

In the chapter 2, I described the detail of experiment. A printing technology and the fabrication method were described. It is also described the analysis methods used in this research.

In the chapter 3, I optimized a printing method by printing process conditions, surface treatment and ITO films.

In the chapter 4, I suggested a hazardous and noxious substances sensor using the ITO layer. The sensor was operated at room temperature without additional heating. Also, we observed the ITO sensing properties under wide pH ranges.

In the chapter 5, I verified the reliability of the fabricated ITO sensor, it was carried out discussion of change and its cause of properties.

Finally, all results were summarized and concluded in the chapter 6.

KEY WORDS: SENSOR, Indium Tin Oxide (ITO), hazardous and noxious substances (HNS), Marine pollution, Environmental monitoring

Chapter 1. Introduction

1.1 Sensor technology

Sensors are detectors that have the ability to measure some type of physical quality that is happening, such as pressure or light. The sensor will be able to convert the measurement into a signal. Most of the sensors in use today are actually going to be able to communicate with an electronic device that is going to be doing the measuring and recording.

Sensors have been used for a long time as the start of the compass to be used from the BC. Since the 1960s, to start using in the industry, the study of sensor technology has been actively deployed. [1] Today, almost people are going to find sensors in a wide range of different devices that you use regularly. The touch screen that you have your smart phone, also you used pressure sensors for opening the doors the market. Sensors are a very common part of everyday life.

Sensor technology is rooted in basic science, it is divided into the sensor devices, sensor system and sensor application technology. Depending on the properties of the object, a physical sensor, a chemical sensor, and the biosensor roughly classified. In modern times, due to splendid development in science and technology, sensor technology development has been made at a phenomenal speed and scale.

Recently, sensor technology combines nanotechnology with MEMS technology. Quickly, data processing and automatic multi-functional smart sensor has been actively being studied. [2] Sensor technology has a simple direction such as performance and production, but now which has developed in trend is divided into eco-friendly, integration, multi-functional, systematic and miniaturization.

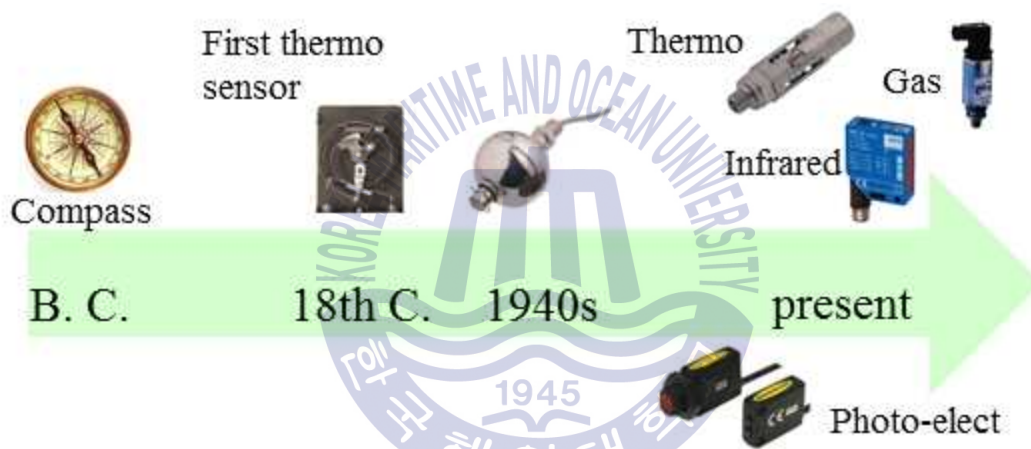


Fig. 1. The history of the sensor development

Figure 1.1 shows the type of sensor that has been developed and studied. [3]

1.2 Sensor technology application

Sensors work in a wide variety of applications in construction, auto-related industries, aerospace, medical fields, environmental monitoring and daily life. Increasing demands for monitoring safety and efficiency being met by solutions development to perform reliably in some challenging environments. But according to industrial level ascends, Even if detecting the information of the object has been developed, without application technique, that sensor may not be worthwhile. Especially, the sensor of human safety and the environment are one of the major application technologies. These sensors are responsible for important role of aircraft, automobiles, ships, disaster prevention technology, and offshore plant safety.

1.2.1 Necessity of hazardous and noxious substances sensor

The 2000 OPRC-HNS Protocol, designed for preparedness and response, defines HNS as a substance other than oil which if introduced into the marine environment is likely to create hazards to human health, to harm living resources and marine life, to damage amenities or to interfere with other legitimate uses of the sea. [3]

The effects of a chemical released into the marine environment will depend on a number of factors such as the toxicity of the material, the quantities involved and the resulting concentrations in the water column, the length of time organisms are exposed to that concentration and the level of tolerance of the organisms. The characteristics of some HNS, particularly heavy metals and some organic compounds, can result in an accumulation of the substances within organisms themselves, a phenomenon known as bio-accumulation. Sessile marine species that filter seawater for food, such as bivalve molluscs, are particularly vulnerable to this problem. Subsequent bio-magnification may also occur if the chemicals can be passed on, following the food chain up to higher predators.

Unlike the oil spills, however, HNS spill issue was not getting the spotlight so far, because chemical spills occur at a much lower frequency than spills of oil. However, the consequence of a chemical spill can be more wide reaching than that of oil and there is growing international awareness of the need for safe and

effective contingency arrangements for chemical spills. The wide variety of chemicals transported, their varying physical and chemical properties, the different ways in which they behave in the environment and the potential for effects on human health mean that response to chemical spills is not as straightforward as for oil. [4]

An Ammonia is one of the substances that utilize maritime transport and commonly used to apply many commercial products. [5] Ammonia has caustic, hazardous, colorless and pungent odor characteristics in its concentrated form. [6] In addition, ammonia creates environmental pollution by forming smog and collapse nitrogen cycle system. Hence, ammonia detection in ocean has an importance.

1.2.2 Current state of HNS sensing technology

HNS detection in ocean has an importance. But there has been no proper sensor for HNS detection in the ocean. While various technologies have been studied for the detection of toxic substances, sensors such as electrochemical gas sensors [7-8], chemiresistor sensors [9], the chemically modified field effect transistor (CHEMFET) sensors [10], optical fiber sensors [11-12] and metal oxide semiconductors sensors [13-16] have attracted substantial attention for the monitoring of toxic substances in gaseous phase as they provide easy and fast means of detection. Among these sensors, metal oxide sensors are of particular interest to the authors of this paper because the metal oxide sensors are compact, require little electric power at the sensing point, relatively inexpensive, available to harsh environment, and environmentally friendly. [17].

1.3 Metal oxide based sensor

Sensors can produce the physically signals and converting the signals into visible data. In order to better measure the change of the target value such as heat, current, pressure, mass etc, sensor devices materials is necessary to understanding of the properties.

Since the phenomenon of photo conductivity was reported by Willoughby Smith (1873), Semiconductor sensor has been a big development in the center of the sensor technology field. However, silicon-based sensor is stable operation in the limited temperature and in applying to various sensors is limited. [18]

Sensor material not only does not change the material properties of the external stimulus, but also there must be selective with respect to other than the target substance of the stimulus. In consideration of such a complex conditions, the sensor materials are enlarged organic, inorganic and composite materials.

Metal oxide is one of major inorganic material. Metal oxide shows a characteristic with stability, high sensitivity and good response. For this reasons that it may be used to control the operating temperature, a number of studies have been conducted as a sensor material.

Metal oxides (ZnO , TiO_2 , SnO_2 , and In_2O_3) have been investigated for various sensors. [11-14] The properties of the theses metal oxide sit is shown in Table1.1. In general, metal oxide sensors reactions such a ionsorption is taking on the surface, it is possible to observe the change in the resistance value of the sensor. which defines the sensitivity of the sensor.

ZnO has a wide band gap of 3.37 eV and high exciton binding energy of 60 meV at room temperature. Also, Shape control is simple, it is an excellent conductive material. However, ZnO is a disadvantage of having a weak durability. TiO_2 is easy to similarly shape control like ZnO , and optical characteristics are excellent. Band gap is limited to visible light at 3.2 eV. Also ZnO has the disadvantage of chemically toxic.

On the other hand, SnO_2 and In_2O_3 have an excellent conductivity and wide band

gap and chemically stable characteristics. For the purpose of application of the sensor material has been much research.

Recently, Many method improved the properties of SnO₂ and In₂O₃, Many researcher studies using ITO which Sn ions are doping in In₂O₃ compensation.

Table 1.1 Summary on characteristic of metal oxide.

	ZnO	SnO₂	In₂O₃	TiO₂
Full name	Zinc Oxide	Tin dioxide	Indium Oxide	Titanium dioxide
Conductive	Good	Good	Good	Bad
Band gap (eV)	3.2	3.8	3.7	3.2
Chemical stability	Weak durability	Good durability	Good durability	Toxicity

1.4 Properties of ITO (Indium Tin Oxide)

Indium tin oxide (ITO) is one of the most widely used transparent conducting oxides because of its two chief properties, it has electrical conductivity and optical transparency. ITO is the compound of In_2O_3 and SnO_2 , it has electrical physical and chemical properties of the two materials. ITO has a band gap energy of $3.5 \sim 3.8$ eV. And the absorption by the inter-band transition in the ultraviolet region, reflection absorption by free electrons in the near-infrared region and high transmittance of more than 85% in the visible light. For In_2O_3 the SN-ion are not doped, oxygen vacancy is formed in a non-stoichiometric composition $\text{In}_2\text{O}_{3-x}$. When the Sn^{4-} ions are added, ITO has N-type semiconductor characteristics in the formation of free electrons. [16]

Properties of Crystallography

ITO is formed an ionic bond to the same crystal structure as the parent phase is In_2O_3 . Crystal structure is a fluorite-related superstructure 1/4 is empty of the position of the anion in the fluorite crystal structure. It was called cubic bixbyite structure, and is composed of 80 atoms (In_2O_3 molecule 16 EA) per Unit Cell. The lattice constant is 10.09, I have a defective inner cations is filled half units 8 are six anions is filled in the position of the anions in the lattice when the oxide is formed. The lattice constant is $10.09 \pm 0.02 \text{ \AA}$, six anions are fill out of the position of the unit cell eight of anion positions, center cation is full of half in When the oxide is formed, it would has a defect. In the ITO crystal structure, it has two different cation positions. [19] The position of the In (1) in Figure 1.2 (b-site, In-O distance: 2.18 \AA), it occupied for 1/4 of the entire cation positions and interstice of the anion is exist. For this reason a distance of anion and cation are the same, and in three directions is a position that receives the same compressive stress by six O^{2-} anion to coordinate. [20]

Meanwhile, The position of the In (2) in Figure 1.2 (d-site, In-O distance: 2.13, 2.19 and 2.23 \AA), it occupied for 3/4 of the entire cation positions and Vacancy of

the position of the anion is exist in the plane's diagonal direction. For this reason a distance of anion and cation are different compressive stress by six O^{2-} anion. The difference in the reason for the In-O defects, repulsion distribution between oxygen ions forming a polyhedron around the In (2) is taken to occur cannot be uniform. Limit the amount of employment of SnO_2 for in_2O_3 is not exactly clear, N. Nadud et al have reported SnO_2 Amount in about 6 to 11%. [21]



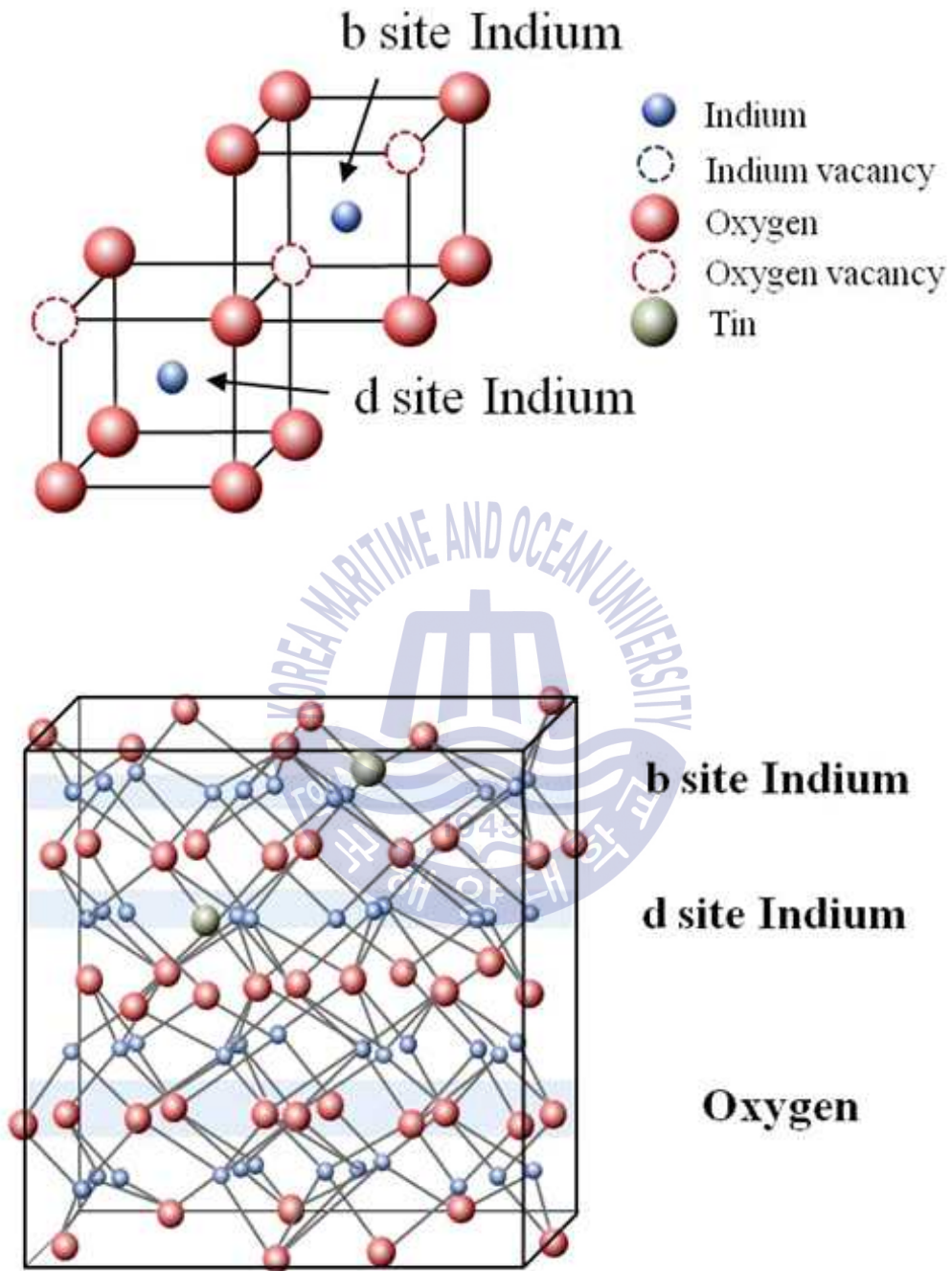


Figure 1.2 Crystal structure of ITO [21]

Properties of Electrical

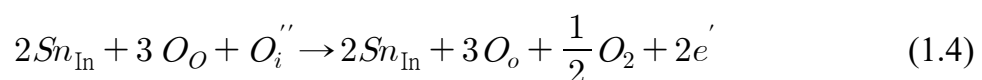
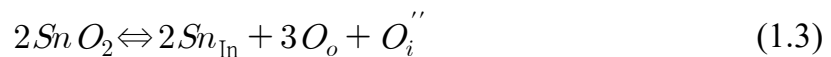
Generally, the electrical conductivity of the material has conductivity (σ). Which may be expressed by Eq. 1.1

$$\sigma = N \mu e \quad (1.1)$$

N is a carrier concentration, μ is mobility and e is electric charge. From Eq 1, in order to obtain high electrical conductivity, we can know that the necessary mobility and high carrier concentration. It is necessary to understanding of the carrier and the mobility that cause the electrically conductive ITO. In the case of ceramic, it has almost of the large band gap and formed a chemically stable stoichiometric composition. So ceramic has electrical insulation Characteristics. However, metal oxides such as ZnO and In_2O_3 has nonstoichiometric composition as Zn_{1+x}O , $\text{In}_2\text{O}_{3-x}$, it is known to shows the electrical conductivity characteristics. $\text{In}_2\text{O}_{3-x}$ is nonstoichiometric composition by the decomposition reaction as Eq 1.2, it has been reported to have N-type conduction properties.



In Eq 1.2, o_o is oxygen, V_O'' is oxygen vacancy, $1/2 O_{2(g)}$ is oxygen of the gas state and e' is electron. However, it is not suitable for use as the conductive film because limited number of carriers generated by the decomposition reaction. Thus, many researcher studies to increase the carrier density by utilizing the method of doping and atmosphere control into nonstoichiometric. A method of add a Sn^{4+} ion, which it is known in the best way.



Eq 1.3 shows the carriers generated by the doping method using In_2O_3 for Sn ions by a chemical formula. Doped Sn^{4+} ions now replace In^{3+} ions, to form a stoichiometric composition, interstitial oxygen in the determination of In_2O_3 is introduced meets the location of the empty oxygen. In other words, the ratio of Sn and O is 2: 1. The introduced oxygen can increase the carrier through a heat

treatment method in a reducing atmosphere as shown in Eq 1.4. (By leading decomposition reaction)

The above mentioned effects, ITO is acting as complex mechanism of electron generation by the carrier generation and oxygen vacancy. At this time, the oxygen vacancies improve the concentration of charge carriers. Excessive oxygen vacancy cause poor mobility of the charge carriers by acting as a defect of the crystalline. In addition, an extra of Sn impurities causes the generation of the unreduced neutral conjugate such as $Sn_2 \cdot O_i''$ and $(Sn_2 \cdot O_4)^x$. Also, it causes a decrease mobility of free electron. Therefore, ITO is Sn doping at In_2O_3 is found to be exist at 6 ~ 11%.

Properties of Optical

ITO has a visible light transmittance higher, so it is widely applied as a photoelectron devices and transparent conducting film. ITO has a wide band gap of above 3.7 eV, it may exhibit two characteristics of the direct transition and the indirect transition. Wide band gap of ITO is free electrons reflection and absorption in the ultraviolet region. And it shows a high transparency in the visible light region. Absorption edge is exist in the UV region, as the concentration of electrons increases and moves to shorter wavelengths. By excess electrons to enter the state of the conduction band, these movements had occurred. It is known as Moss-Burstein shift. [22] It is possible to know the energy through the movement of these absorption edges. This property, ITO blocks the visible light and shows a high absorption in UV.

Based on ITO layer

Metal oxide semiconductor has a wide band gap and a good electrical conductivity, and applicable as optical devices and sensor. When the metal oxide is applied to the sensor, which is excellent in stability and robustness. So many studies have been conducted. If the structure is different. Not only the different physical properties, but also different other properties when applied to the materials.

In Table 1.2, we compared the characteristics of different structural characteristics ITO sensor. ITO thin-film sensor was fabricated by using Sputter. It exhibits excellent electrical characteristics with low specific resistance value and high mobility. These electrical properties, reactivity of the sensor were not good. The improvement part of sensitivity has continued to be pointed out. In comparison, ITO nano powders sensor was fabricated by using printing coat process. Electrical characteristics are not excellent, but I have shown the possibility of good sensitivity by wide specific surface area. Although high reactivity in the essential characteristics is required as a sensor, also it needs to consider the safety and application range.

I was observing the changes in the surface temperature of when the two different structural characteristics sensors. As a result, ITO thin-film sensors showed a change in surface temperature of 100°C or more rises at 5V. On the other hand, ITO nano powders sensors showed no significant change the surface temperature rises even at high voltage 30V. For this reason, it can be known that the form of ITO powder is a suitable structure for stably operated at room temperature.

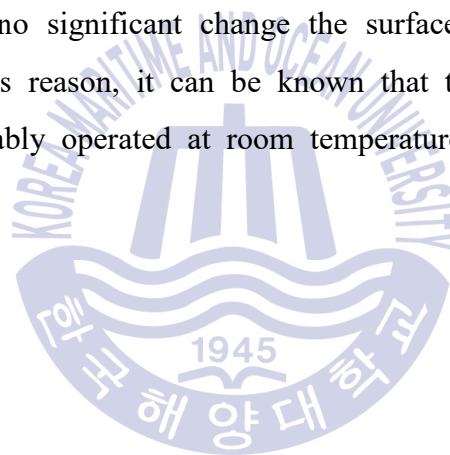
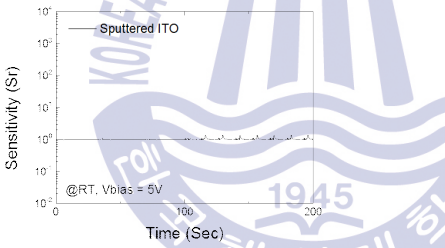
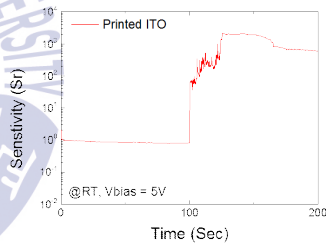
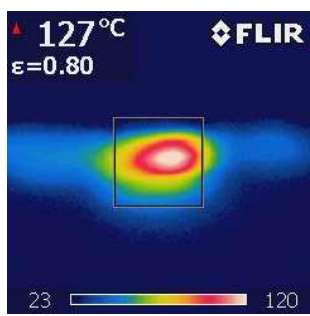
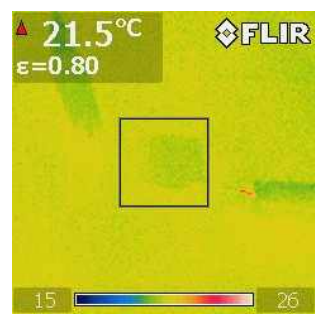


Table 1.2 Sensor properties of ITO compared by structure

Structure	ITO film [23]	ITO nano-powder [24]
Fabrication	Sputter	Printing process
Electrical Properties	<p>Low resistivity (26 Ω/\square)</p> <p>High mobility (20~30 cm^2/VS)</p>	<p>High resistivity (109k Ω/\square)</p> <p>Low mobility (0.01~10 cm^2/VS)</p>
Sensor property	<p>Bad response</p> 	<p>Good response</p> 
Thermal property	 <p>$V_{\text{bias}} = 5\text{V}$ Current = 0.3A Temperature = 127°C</p>	 <p>$V_{\text{bias}} = 30\text{V}$ Current = 0.25 μA Temperature = 22°C</p>

1.5 Proposal and purpose of this study

In this study, I proposed a new Hazardous Noxious Substances (HNS) sensor for the spill and disaster prevention. I need high stability and reliability sensor materials to the my purpose. I proposed to develop a hazardous substance sensor operable at room temperature without heating devices.

I using the ITO nano powder for the fabrication of the sensor, because ITO nano powder has high reactivity, chemically stable and wide surface area. Utilizing printing coat techniques, I attempted to fabricate the ITO layer sensor.



Reference

- [1] <http://what-is-a-sensor.com/who-invented-the-first-sensor/>
- [2] Sailor, Michael J., and Jamie R. Link. "'Smart dust': nanostructured devices in a grain of sand." *Chemical Communications* 11 (2005): 1375-1383.
- [3] International Maritime Organization. "Protocol on Preparedness, Response and Co-operation to pollution Incidents by Hazardous and Noxious Substances, 2000 (OPRC-HNS Protocol)".
- [4] Lee, Moonjin, and Jung-Yeul Jung. "Risk assessment and national measure plan for oil and HNS spill accidents near Korea." *Marine pollution bulletin* 73.1 (2013): 339-344.
- [5] Are HNS Spills more Dangerous than Oil Spills?: ITOPF, <http://www.itopf.com/> (accessed May 2014).
- [6] Toxic FAQ Sheet for Ammonia: Agency for Toxic Substances and Disease Registry, <http://www.atsdr.cdc.gov/tfacts126.pdf> (accessed September 2004)
- [7] Yen-te Chao, William J. Buttner, et al. "HYDROGEN AMPEROMETRIC GAS SENSOR: PERFORMANCE EVALUATION BY SSTUF." *Chemical Sensors VI: Chemical and Biological Sensors and Analytical Methods: Proceedings of the International Symposium*. Vol. 2004. The Electrochemical Society, 2004.
- [8] Ho, Clifford K., and Charles F. Lohrstorfer. "In situ monitoring of vapor phase TCE using a chemiresistor microchemical sensor." *Groundwater Monitoring & Remediation* 23.4 (2003): 85-90.
- [9] Krishna, T. Vamsi, et al. "Modeling and design of polythiophene gate electrode ChemFETs for environmental pollutant sensing." *University/Government/Industry Microelectronics Symposium, 2003. Proceedings of the 15th Biennial. IEEE, 2003.*
- [10] Cao, Wenqing, and Yixiang Duan. "Optical fiber-based evanescent ammonia sensor." *Sensors and Actuators B: Chemical* 110.2 (2005): 252-259.
- [11] Comini, E., and G. Sberveglieri. "Metal oxide nanowires as chemical sensors."

Materials Today 13.7 (2010): 36-44.

- [12] Tian, Wei-Cheng, et al. "Sensing performance of precisely ordered TiO₂ nanowire gas sensors fabricated by electron-beam lithography." Sensors 13.1 (2013): 865-874.
- [13] Yu-De, Wang, et al. "Electrical and gas-sensing properties of WO₃ semiconductor material." Solid-State Electronics 45.5 (2001): 639-644.
- [14] Park, Jae Young, Dong Eon Song, and Sang Sub Kim. "An approach to fabricating chemical sensors based on ZnO nanorod arrays." Nanotechnology 19.10 (2008): 105503.
- [15] Li, Chao, et al. "In₂O₃ nanowires as chemical sensors." Applied Physics Letters 82.10 (2003): 1613-1615.
- [16] Nistor, M., et al. "Nanocomposite indium tin oxide thin films: formation induced by a large oxygen deficiency and properties." Journal of Physics: Condensed Matter 22.4 (2010): 045006.
- [17] Liu, Xiao, et al. "A survey on gas sensing technology." Sensors 12.7 (2012): 9635-9665.
- [18] Jung, Ji-Chul, and Sang-Mo Koo. "The Effect of Catalytic Metal Work Functions and Interface States on the High Temperature SiC-based Gas Sensors." Journal of the Korean Institute of Electrical and Electronic Material Engineers 24.4 (2011): 280-284.
- [19] Walsh, Aron, et al. "Physical properties, intrinsic defects, and phase stability of indium sesquioxide." Chemistry of Materials 21.20 (2009): 4962-4969.
- [20] Mukhopadhyay, Saikat, et al. "Theoretical study of small clusters of indium oxide: InO." Journal of Molecular Structure: THEOCHEM 948.1 (2010): 31-35.
- [21] Nadaud, N., et al. "Structural studies of tin-doped indium oxide (ITO) and In₄Sn₃O₁₂." Journal of Solid State Chemistry 135.1 (1998): 140-148.
- [22] Fujiwara, Hiroyuki, and Michio Kondo. "Effects of carrier concentration on

the dielectric function of ZnO: Ga and In₂O₃: Sn studied by spectroscopic ellipsometry: analysis of free-carrier and band-edge absorption." Physical Review B 71.7 (2005): 075109.

[23] Vaishnav, V. S., P. D. Patel, and N. G. Patel. "Indium tin oxide thin film gas sensors for detection of ethanol vapours." Thin solid films 490.1 (2005): 94-100.

[24] Yang, M. et. al. 2009. Characteristics of single neurons cultured on microelectrode arrays in vitro for chemical sensing, Institute of Electrical and Electronics Engineers, 5, pp.690-695.



Chapter 2. Experimental methods

2.1 Film printing method

The print technology is the electronic circuit board or electronic circuits by using a functional ink. And using this print methods, a field of study of various printing techniques. For example, when printing a display or electronic devices on a flexible substrate such as plastic, it is applicable is the display which can be bent. Utilizing the printing technologies, it simplifies the existing processes, the productivity is improved. For properties that can be diversity of materials such as organic, inorganic and metal, application areas are a variety of known that. [1]

Screen printing

Screen printing is a printing technique whereby a mesh is used to transfer ink onto a substrate, except in areas made impermeable to the ink by a blocking screen. Screen printing, the loss of material is small process. Studies for the manufacture of displays, such as PDP or OLED has been advanced. [2, 3]

Screen uses a stainless steel and teflon for fine patterning. For proper viscosity of the ink paste used it is necessary, it is used as a binder by dispersing a resin and a solvent to the basic material. Process using a screen printing method, it is shown in Fig 2.1. Screen printing is performed via the four basic processes. (Rolling, jetting, removal of the screen and leveling) [4, 5]

Rolling: Rolling is the role of stabilizing the constant paste and the viscosity on the screen. It is an important process for obtaining a uniform thin film.

Jetting: Paste is pushed paste by Squeegee and passing between the screen mask is a process of exiting pushed the substrate surface. Affected by the angle and power of Squeegee.

Removal of the screen: After reaching the paste the substrate surface, it is a stage where the screen unstocks on the substrate. It is an important process in determining the continuous printing property and resolution.

Leveling: After Removal of the screen, it can maintain the shape with its force (surface tension) paste on a substrate, and a process of forming a pattern in

accordance with the lack of the substrate.

If these basic process variable is fixed, it can affect print resolution is pasted and screen mask, which requires appropriate adjustments accordingly. By properly adjusting the concentration of the paste, it is possible to pattern even less than the minimum line width of 10~20 um. [6]



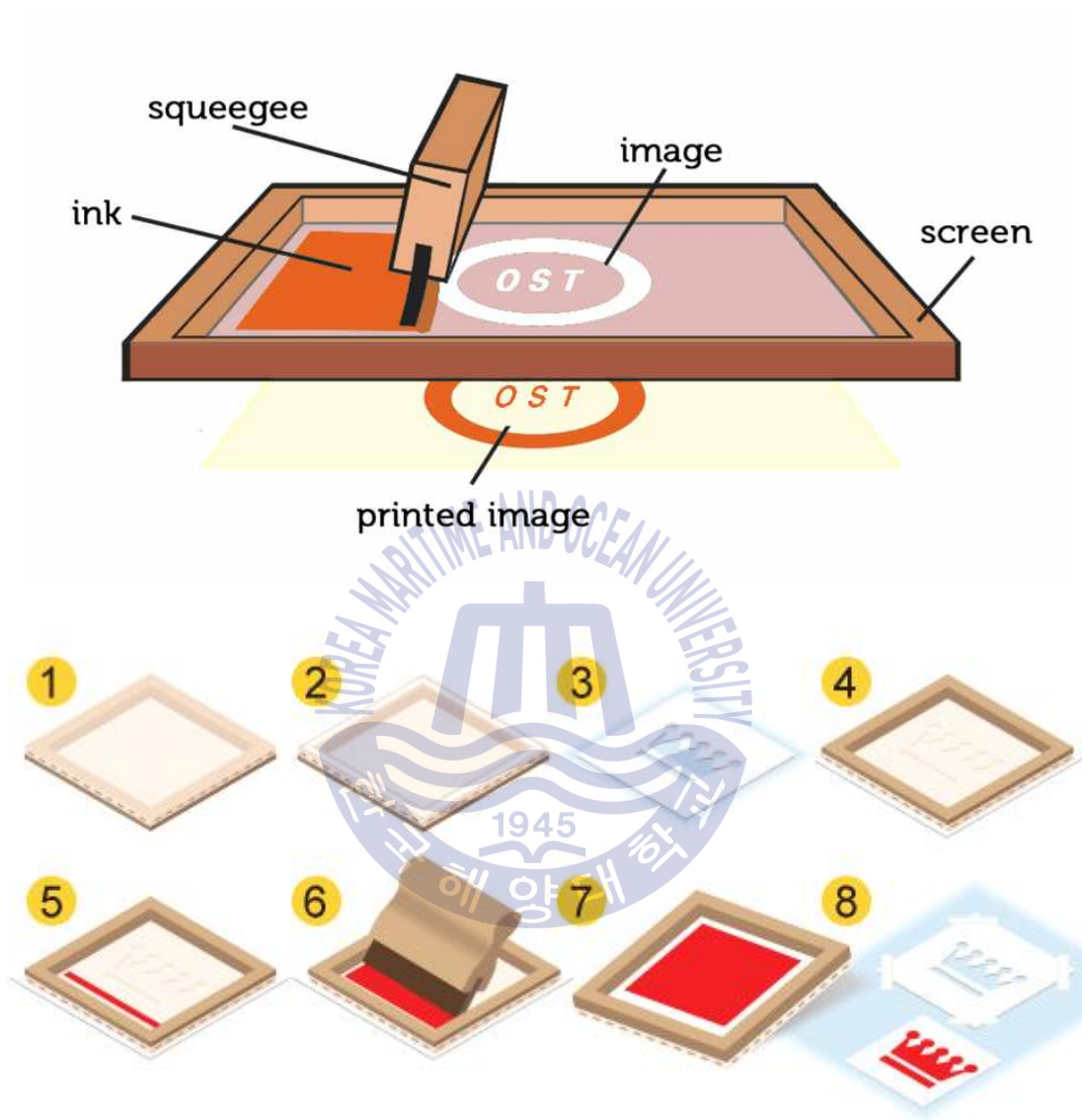


Figure 2.1 Schematic diagram of screen-printing process.

2.2 ITO layer printing

ITO layer is by using the ITO nano powder was fabricated by screen printing method. Fig. 2.2 shows the photograph of screen printing process. Screen printed ITO layer is manufactured in four steps as follows.

(1) Paste making: We made a paste for screen printing that contains the ITO nano-crystals and organic binder with 1:1 weight ratio. Fabricated ITO pastes those shown in Figure 2.2 (a).

(2) Substrate surface treatment: In this experiment, we were using a quartz (SiO_2) substrate. The size of the substrate is about $35 \times 35 \text{ mm}^2$ with a thickness of 1mm. The quartz substrate shown in Figure 2.2 (b) is surface treated, which were cleaned sequentially with methanol, acetone and DI water in an ultrasonic bath to remove organics and impurities on the surface, where each step took 15 minutes.

(3) Screen printing: We were printed using serpentine pattern mask on substrates to increase the resistance of ITO electrode in confined area. ITO nano-crystals were printed using a zigzag-pattern mask on a treated quartz substrate to increase the resistance of ITO electrode in confined area. Figure 2.2 (c) is the photograph of the screen-printer.

(4) Debinding organic binder: After screen printing, in order to remove the organic binder of printed ITO layers, we were using an electric furnace as shown in Figure 2.2 (d). The ITO layer was heated at $200 \text{ }^\circ\text{C}$ for 1.5 hour to remove volatile organic solvent. Because, it remove only organic binder, in order to confirm that no change has crystallinity and shape of the surface morphology, cellulose is decomposed at $200 - 250 \text{ }^\circ\text{C}$. [7] But, It will change the surface morphology or crystallinity ITO at $300 - 400 \text{ }^\circ\text{C}$. This is because to act as an annealing treatment to ITO layer surfaces. [8, 9]

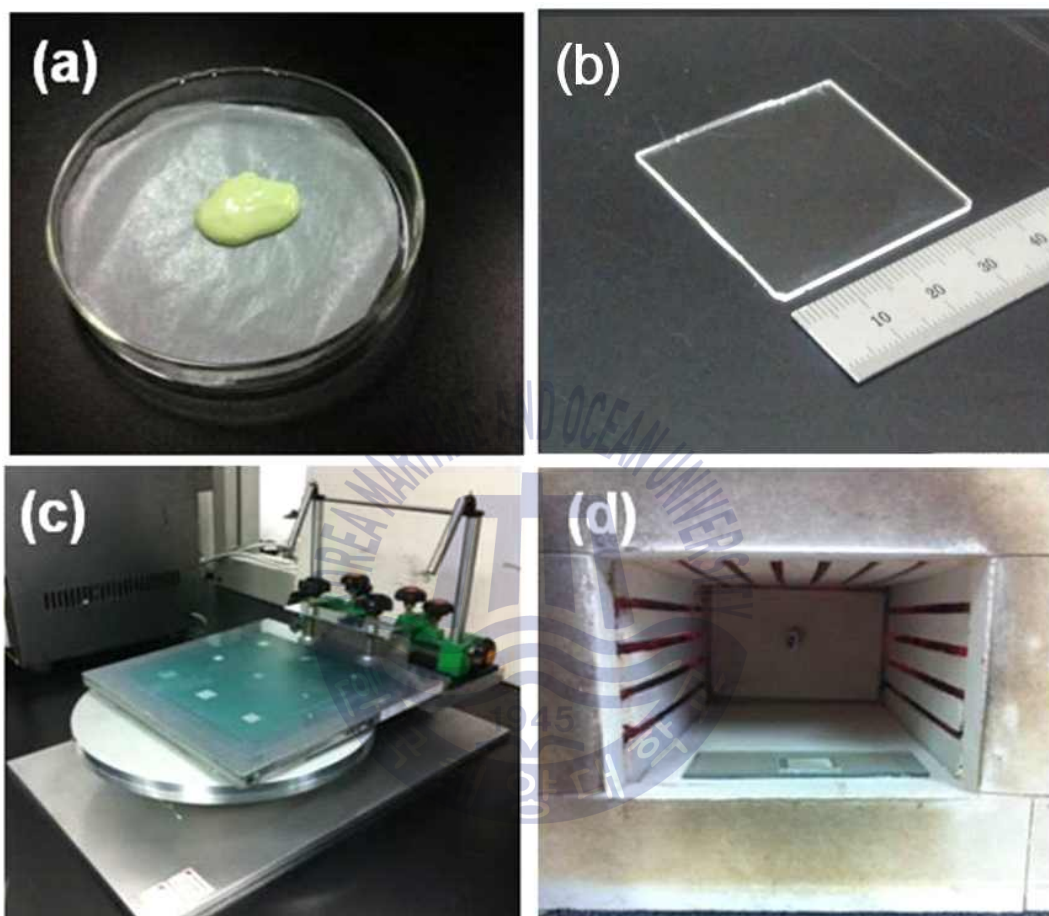


Figure 2.2 Summary of the screen printing process and experimental apparatus. (a) fabricated ITO pates, (b) substrate after cleaning, (c) screen printing, (d) furnace for debinding

2.3 Characterization Methods

2.3.1 Optimization of ITO layer

In this section, in order to confirm the optimized conditions of the printed ITO layer, to observe the surface energy of the substrate which is surface treated. It confirmed the optimization of the layer by surface treatment.

I was using the Sessile Drop contact angle analyzer in the method of measuring the surface energy. And, In order to observe the surface of the printed layer was used for Optical microscope.

Sessile Drop method

The Sessile Drop Technique is a method used for the characterization of solid surface energies, and in some cases, aspects of liquid surface energies. The contact angle is defined as the angle made by the intersection of the liquid/solid interface and the liquid/air interface. It can be alternately described as the angle between solid sample's surface and the tangent of the droplet's ovate shape at the edge of the droplet. A high contact angle indicates a low solid surface energy or chemical affinity. This is also referred to as a low degree of wetting. A low contact angle indicates a high solid surface energy or chemical affinity, and a high or sometimes complete degree of wetting. [4] For example, a contact angle of zero degrees will occur when the droplet has turned into a flat puddle; this is called complete wetting. In this study, I was confirmed surface energy in the Static Contact angle method that utilizes a contact angle of Liquid drop, as shown Fig2.3. [10]

Fig 2.3 shows, when the droplet contacts the solid surface shows good contact angle formation between the liquid and the solid. The formation of these contact angles may be determined surface energy through the equilibrium thermodynamic interfacial energy.

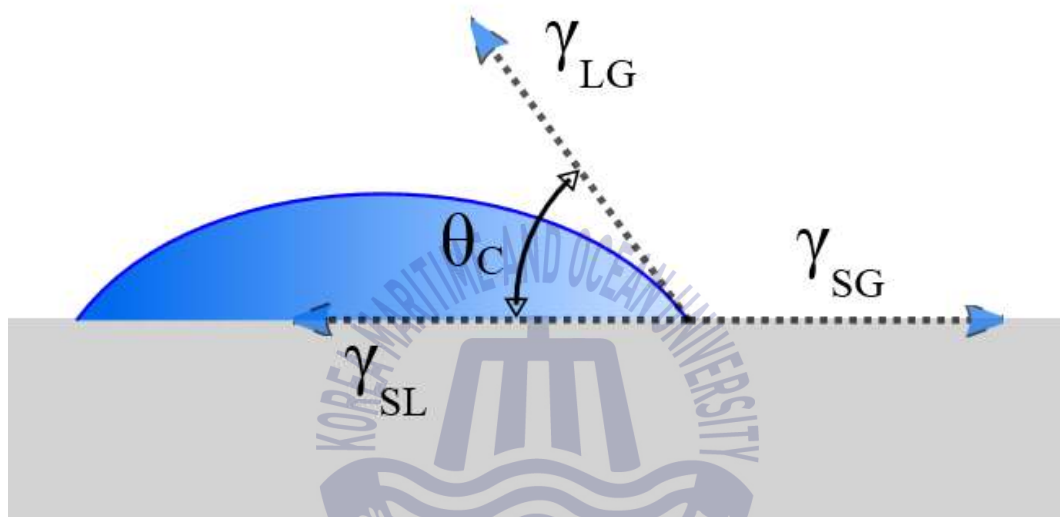


Figure 2.3 An illustration of the sessile drop technique with a liquid droplet partially wetting a solid substrate. θ_c is the contact angle, and γ_{SG} , γ_{LG} , γ_{SL} represent the solid-gas, gas-liquid, and liquid-solid interfaces, respectively.

Optical microscope: OE

The optical microscope, often referred to as light microscope, is a type of microscope which uses visible light and a system of lenses to magnify images of small samples. Resolution is several micro. It does not require surface treatment and is able to measure at ambient conditions. By measuring the phase or reflectance of the light reflected on the sample, it is possible to measure the structure of the surface, the thickness of the thin film.

OE can observe the magnified image using a condensor lens, an objective lens, and a projector lens. Condensor lens is focusing the light source is injected to the surface. Connecting the injected light has been expanded through the objective lens real image. And it is possible to observe a magnified image through the projector lens. These principles is shown in Figure 2.4.



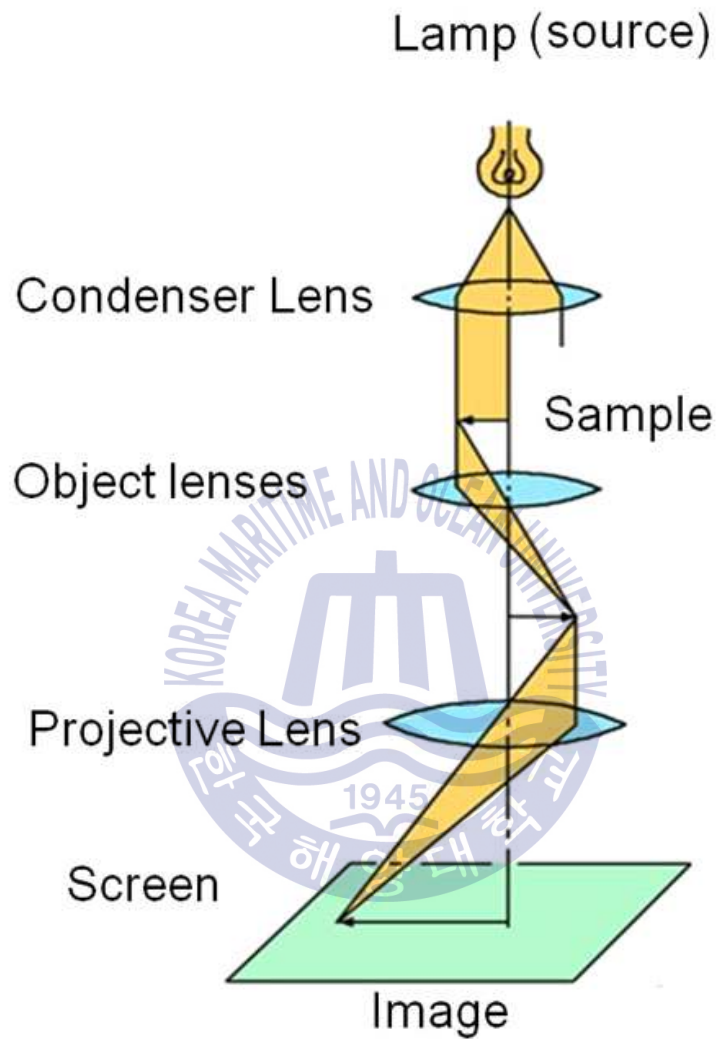


Figure 2.4 Schematic diagram of optical microscope

2.3.2 Surface and material properties of printed layers

In this chapter, in order to observe the surface shape of the printed film, we use field-emission scanning electron microscopy and transmission electron microscopy. In addition, we use the x-ray diffraction to observe the structure and use photoluminescence to observe the crystallinity.

Field-emission scanning electron microscopy: FE-SEM

A FE-SEM is a microscope that works with electrons (particles with a negative charge) instead of light. These electrons are liberated by a field emission source. The object is scanned by electrons according to a zig-zag pattern. FE-SEM is used to visualize very small topographic details on the surface of entire or fractioned objects. Researchers in biology, chemistry and physics apply this technique to observe structures that may be as small as 1 nanometer.

Electrons are liberated from a field emission source and accelerated in a high electrical field gradient. Within the high vacuum column these so-called primary electrons are focused and deflected by electronic lenses to produce a narrow scan beam that bombards the object. As a result secondary electrons are emitted from each spot on the object. The angle and velocity of these secondary electrons relates to the surface structure of the object. A detector catches the secondary electrons and produces an electronic signal. This signal is amplified and transformed to a video scan-image that can be seen on a monitor or to a digital image that can be saved and processed further.

Figure 2.5 illustrates the operating principle of the FE-SEM. FE-SEM uses a field-emission gun instead of a thermal electron gun. Because it uses the electron beam emitted when forming a strong electric field on the metal surface, the brightness is good and resolution is improved. Secondary electrons are used in the secondary electron detector, a photon electronic strong energy is generated by hitting the scintillator is introduced into a photomultiplier tube. Secondary electrons not only for bandwidth spacious are electron production of about 10^5 - 10^6 , but also backscattered electrons also be detected. Electrons emitted by the electron beam to observe the surface of the sample. Then, FE-SEM signaling information of the secondary electrons to the electron detector, after being amplified, we would be observed on CRT.

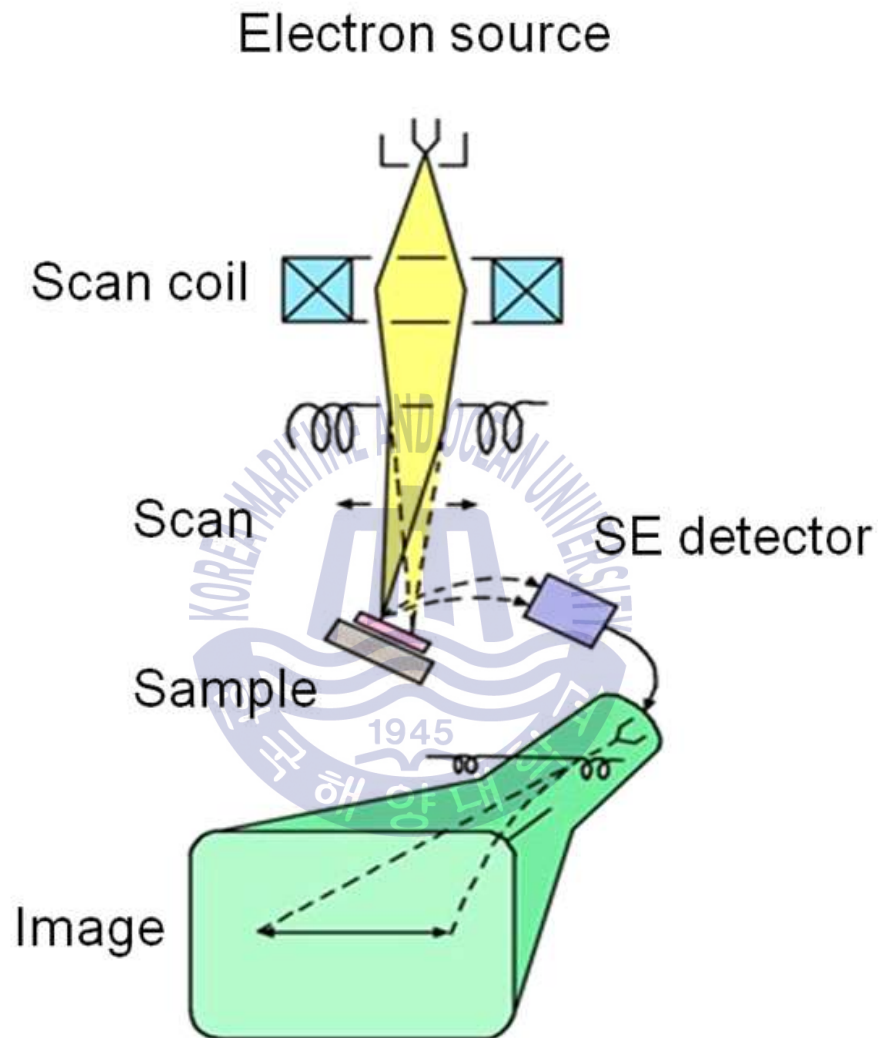


Figure 2.5 Schematic of diagram of SEM

Transmission electron microscopy: TEM

The transmission electron microscopy (TEM) is a powerful tool for material science. A high energy beam of electrons is shone through a very thin sample, and the interactions between the electrons and the atoms can be used to observe features such as the crystal structure and features in the structure like dislocations and grain boundaries. Chemical analysis can also be performed. TEM can be used to study the growth of layers, their composition and defects in semiconductors. High resolution can be used to analyze the quality, shape, size and density of quantum wells, wires and dots.

The TEM operates on the same basic principles as the light microscope but uses electrons instead of light. Because the wavelength of electrons is much smaller than that of light, the optimal resolution attainable for TEM images is many orders of magnitude better than that from a light microscope. Thus, TEMs can reveal the finest details of internal structure - in some cases as small as individual atoms (1~2 Å).

As the electrons pass through the sample, they are scattered by the electrostatic potential set up by the constituent elements in the specimen. After passing through the specimen they pass through the electromagnetic objective lens which focuses all the electrons scattered from one point of the specimen into one point in the image plane. Also, shown in fig 2.6 (b) is a dotted line where the electrons scattered in the same direction by the sample are collected into a single point. This is the back focal plane of the objective lens and is where the diffraction pattern is formed.

TEM can check the shape of the specimen, structural, and distribution binds and image analysis function. And Decision analysis using diffraction, has a function to measure the elemental qualitative measurement.

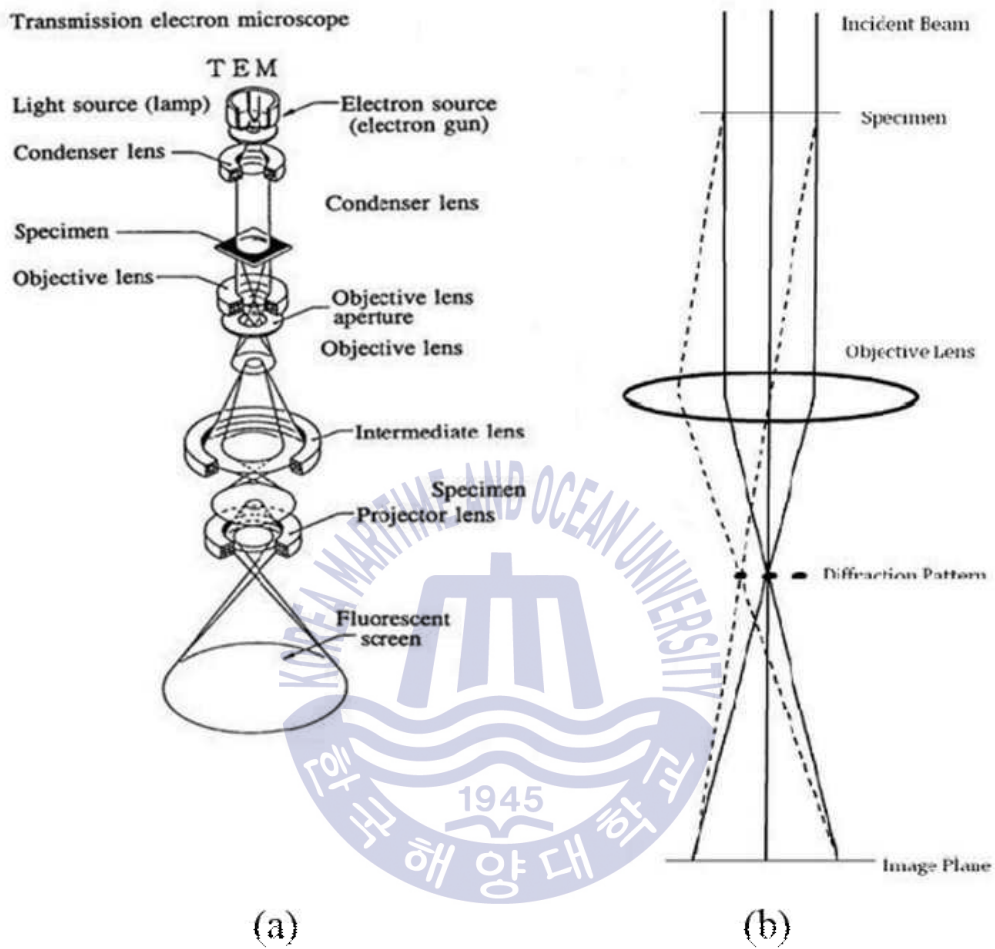


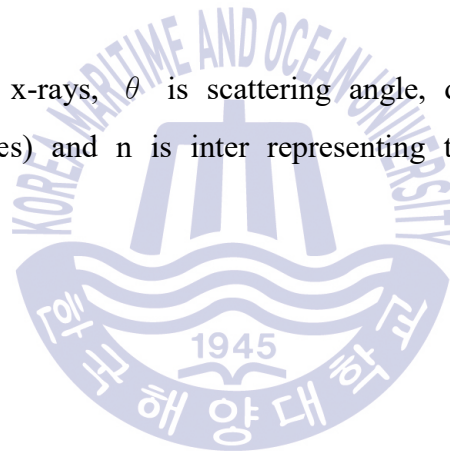
Figure 2.6 (a) Schematic diagram of TEM (b) A ray diagram for the diffraction mechanism in TEM [11]

X-ray diffraction: XRD

X-ray diffraction (Fig 2.7) is widely used in measuring the crystal structure as an important analysis method. X-ray have wavelengths on the order of a few angstroms (1 Angstrom = 0.1nm). This is the typical inter-atomic distance in crystalline solid; making X-rays are scattered from a crystalline solid they can constructively interface, producing a diffracted beam. The relationship describing the angle at which a beam of X-ray of a particular wavelength diffracts from a crystalline surface was discovered by Sir William H. Bragg and Sir W. Lawrence and is known as Bragg's law. As it is shown in fig 2.8, the planar interface 1, 2, and 3

$$2d \sin \theta = n \lambda$$

λ is wavelength of x-rays, θ is scattering angle, d is inter-plane distance of (i.e. atoms, ions, molecules) and n is inter representing the order of the diffraction peak.



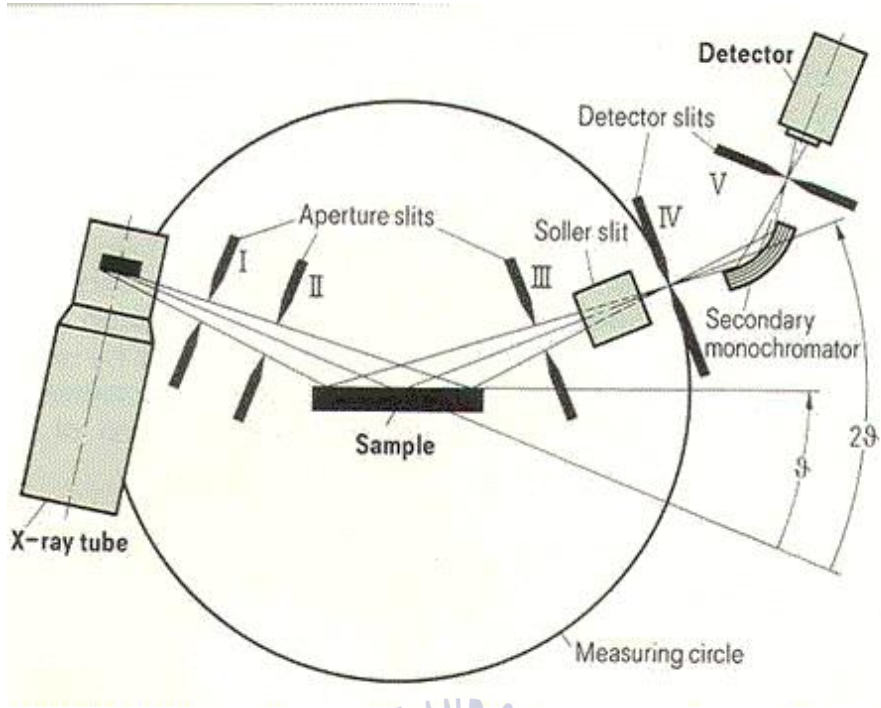


Figure 2.7 X-ray diffraction diagram

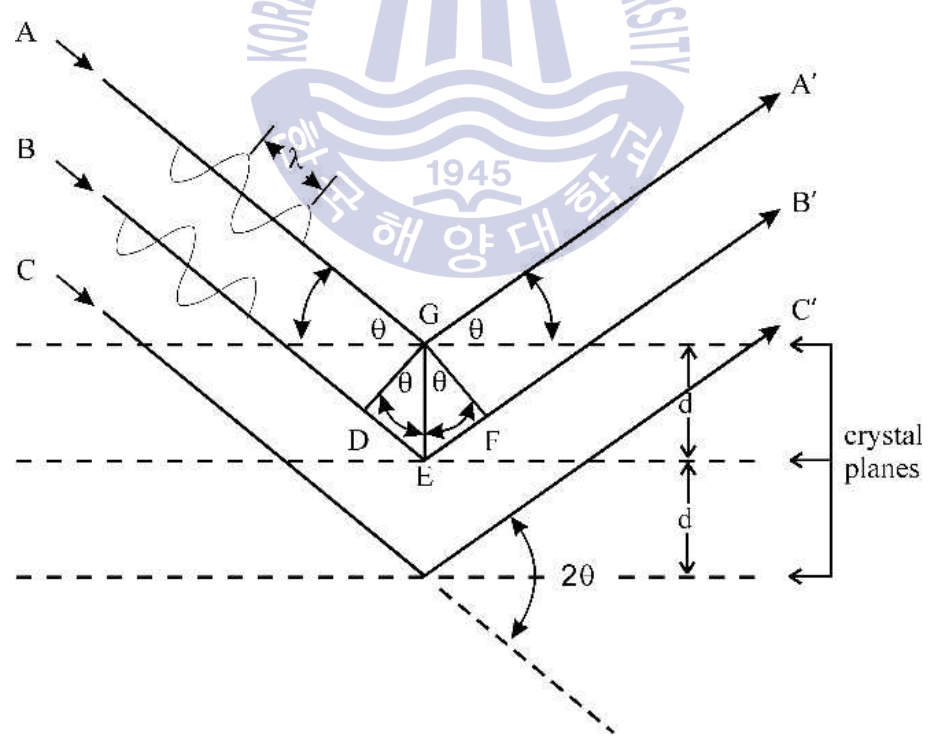


Figure 2.8 Bragg's law

Photoluminescence: PL

Photoluminescence is an important technique for measuring purity and crystalline quality of semiconductors such as ZnO and GaA, especially in electrical structure. PL is a process in which a substrate absorbs photons (electromagnetic radiation) and then re-radiated photons. Quantum mechanically, this can be described as an excitation to a higher energy state and then a return to a lower energy accompanied by the emission of a photon corresponding to various recombination process in figure 22. During this process, there are six different kinds of recombination structure with emitting photons: free carrier recombination, free exciton recombination, bound exciton recombination, shallow level and Eigen inter-band carrier recombination, acceptor-donor recombination and SHR recombination, which were related to the electronic structure, such as binding energy, exciton level, donor level and so on. Therefore, the PL process contains rich information of material structure and components in the material.



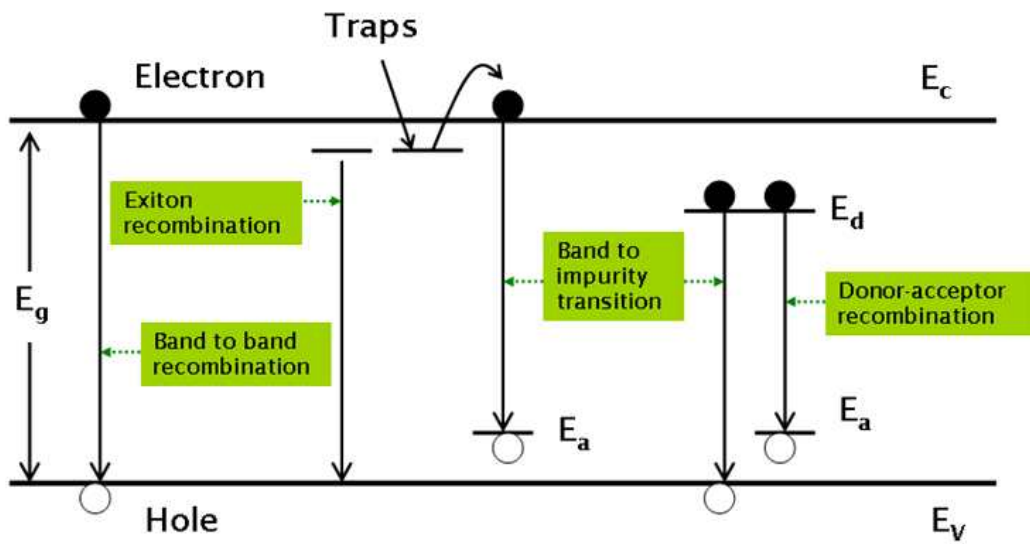


Figure 2.9 Recombination process of Photoluminescence spectra

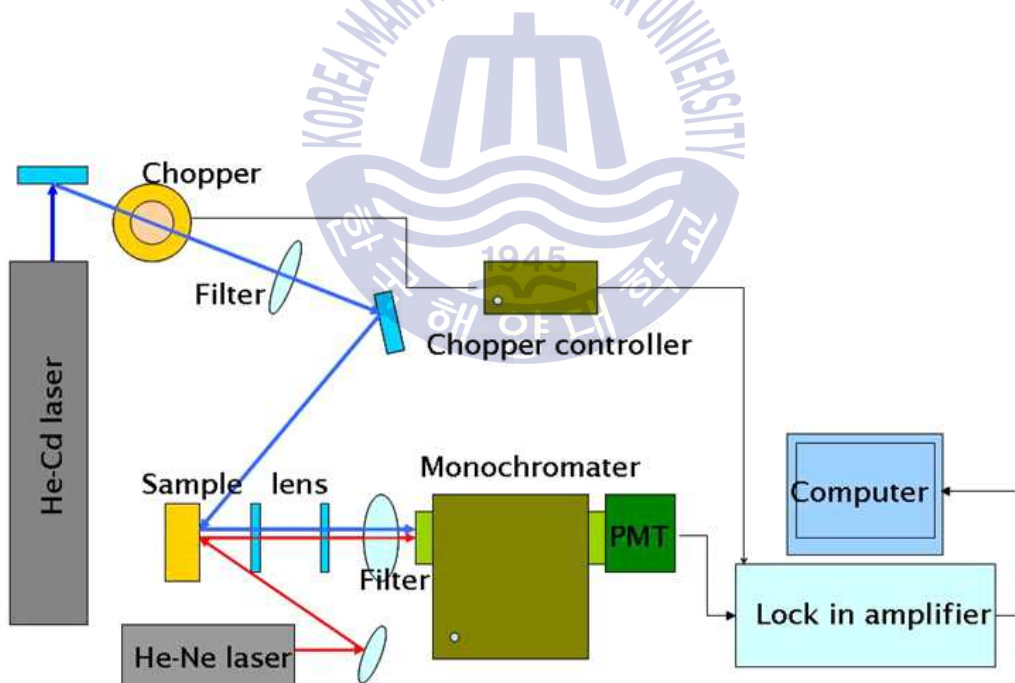


Figure 2.10 Schematic diagram of Photoluminescence

Current-voltage measurement: I-V measurement

A current-voltage characteristic or I-V curve (current-voltage curve) is a relationship, typically represented as a chart or graph, between the electric current through a circuit, device, or material, and the corresponding voltage, or potential difference across it.

It was used IV measuring method to observe the resistance change of the crafted layer. Current and power supply and measurement was determined to constitute a Keithley 2400V instrument as Fig2.10.

Current and voltage graphs may represent the amount of change in a linear manner as shown in Equation 2.1.

$$y = mx + b \quad (2.1)$$

Y is the dependent variable, x is the independent variable, m is the slope, b is the y-axis intercept. When the straight line of the coordinate passes through the origin, y-axis intercept is 0. It can be expressed as Equation 2.2. This formula is in the form such as Ohm's law.

$$I = \frac{V}{R} \quad (2.2)$$

The dependent variable is current, independent variable is a voltage, and the slope is inversely proportional to the resistance. The measured current voltage is displayed as shown in Figure 2.11. In general, characteristics of the device are defined in the characteristic curve of the correlation between the characteristics of the two variables.

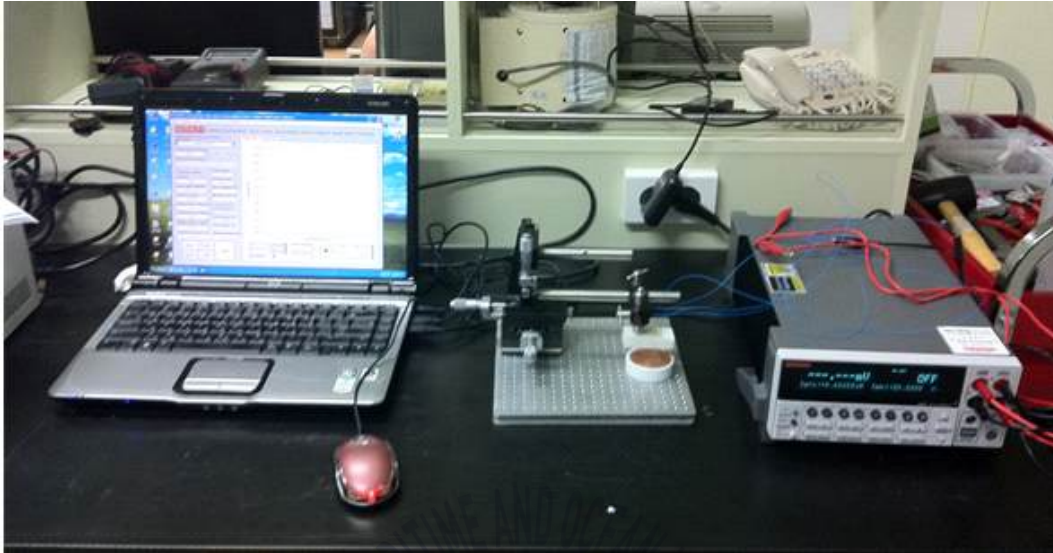


Figure 2.11 Current-voltage measurement

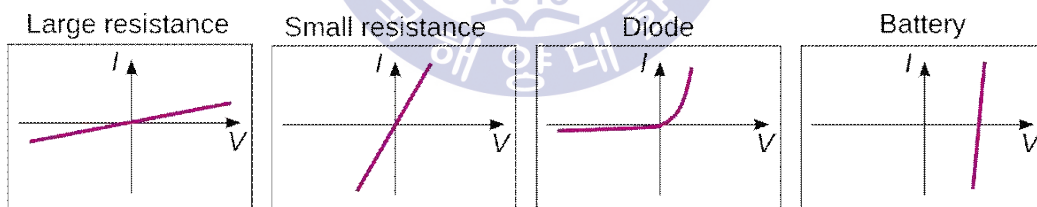


Figure 2.12 Characteristic of current-voltage

4-probe measurement

In using the Napson's resistance measuring system in order to measure the conductivity of thin film, it was 4 probe measurement. 4 probe measuring method, as shown in Fig2.13, tips of four terminals are spaced at regular intervals. It current to the terminals 1 and 2, by measuring the voltage between the terminals 2 and 3, to calculate the resistance by using the ratio between voltage and current. Surface resistance can be calculated as shown in Eq 2.3. (T) is thickness, (W) is width and (L) is length.

$$R = \rho \frac{L}{WT} = \frac{\rho}{T} \frac{L}{W} = \rho_s \frac{L}{W} \quad (2.3)$$



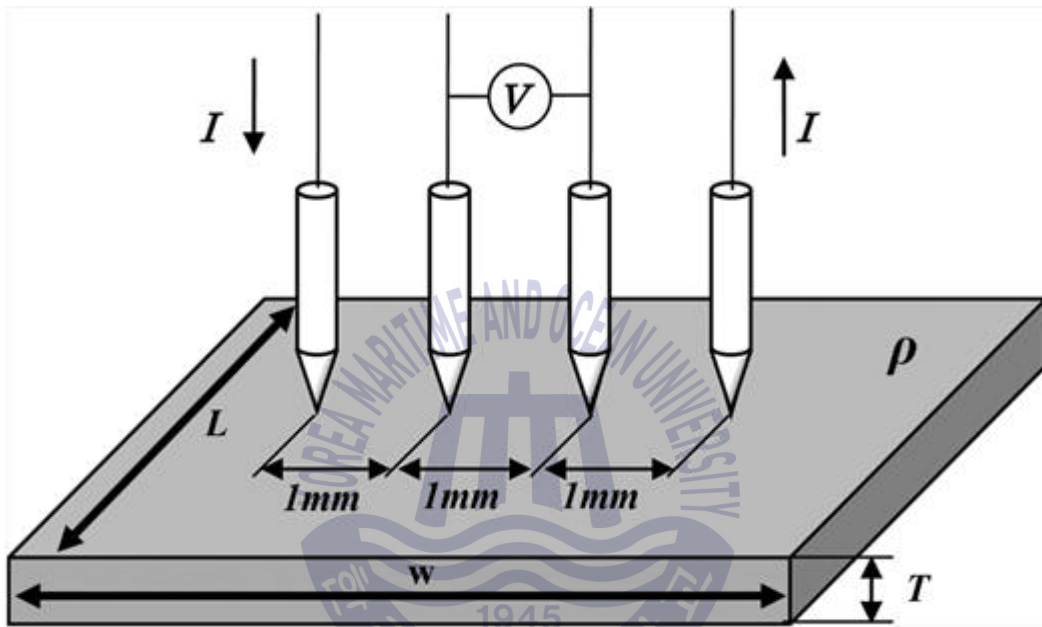


Figure 2.13 Description of 4 - probe measurement

2.3.3 Sensor performances

In this experiment, I was evaluated of the sensor was experimentally from the water bath as shown in Figure 2.14. The electrode was advanced by connecting with silver paste on the sample stage. The change in resistance was confirmed using a Keithley 2400V instrument. It was carried out the operation evaluation as HNS sensor with aqueous ammonia. After with the 100-second settling time, I flowed up 5-25% of ammonia at 5% intervals. In addition, In order to confirm the selectivity, we were carried out experiments in the pH buffer solution.



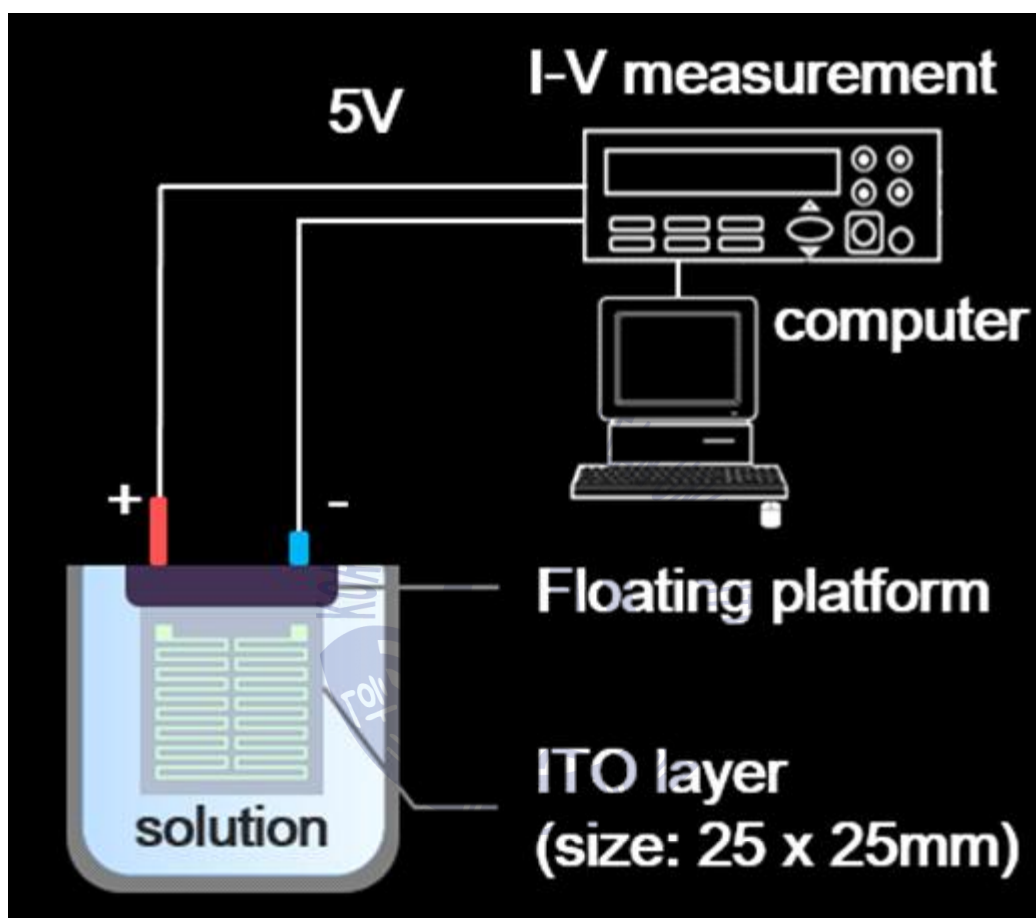


Figure 2.14 Schematic diagram of ITO layer sensor measurement.

Reference

- [1] Perelaer, Jolke, et al. "Printed electronics: the challenges involved in printing devices, interconnects, and contacts based on inorganic materials." *Journal of Materials Chemistry* 20.39 (2010): 8446-8453.
- [2] Lee, D-H., et al. "Screen-printed white OLED based on polystyrene as a host polymer." *Current Applied Physics* 9.1 (2009): 161-164.
- [3] Deng, Jiang, et al. "The Fabrication of Screen-Printed Lanthanum Hexaboride Films Applied in PDP Protective Layer." *Advanced Materials Research*. Vol. 815. 2013.
- [4] 이미영, 스크린 인쇄법에 의한 유기 박막 트랜지스터 제작 및 물성 연구, 박사 학위 논문, 부산; 부산대학교
- [5] 임종선, et al. "인쇄전자소자: 고해상도 인쇄공정기술의 현황 및 전망." *Polymer Science and Technology* 18.3 (2007).
- [6] Zhang, Tengyuan, et al. "Fabrication of flexible copper-based electronics with high-resolution and high-conductivity on paper via inkjet printing." *Journal of Materials Chemistry C* 2.2 (2014): 286-294.
- [7] Shafizadeh, Fred, and A. G. W. Bradbury. "Thermal degradation of cellulose in air and nitrogen at low temperatures." *Journal of Applied Polymer Science* 23.5 (1979): 1431-1442.
- [8] Liu, Xiao, et al. "A survey on gas sensing technology." *Sensors* 12.7 (2012): 9635-9665.
- [9] Nistor, M., et al. "Nanocomposite indium tin oxide thin films: formation induced by a large oxygen deficiency and properties." *Journal of Physics: Condensed Matter* 22.4 (2010): 045006.
- [10] https://en.wikipedia.org/wiki/Sessile_drop_technique
- [11] <https://www2.warwick.ac.uk/fac/sci/physics/current/postgraduate/regs/mpags/ex5/techniques/structural/tem/>

Chapter 3. Characteristics of ITO film by printing coat method

Printing technology is utilized with a variety of devices, printing technique and substrate in the industrial sector. In general, In order to apply printing technology should fabrication of devices with superior pattern takes precedence. [1, 2]

Common matters in all printing techniques, it is intended that the ink moves to the solid surface, and to implement the desired shape of the printed pattern. When contacted with ink and surface, it is an important technique of modulating the interaction of the substrate surface of the ink. This interaction can be classified into two types.

First, it is intended to regulate the surface energy of the substrate surface. In order to adjust the surface energy, studies with a chemical treatment, plasma treatment and microstructure on the solid surface is in progress. This surface energy under the influence of the substrate properties, and it is constrained in the fabrication process. [3]

Second is to regulate the physical properties of the ink. The shape of the pattern, the thickness varies depending on the physical properties of the ink. When it changes to the shape change and the thickness of the printing pattern, electrical characteristics of pattern is changed. [4] Therefore, in order to implement the printing film of excellent quality, it is necessary to study to control the solid surface energy and properties of pastes.

In Chapter 3, to implement the printing film of excellent quality, it is desired to control the ink physical properties and the surface energy on the substrate. And then, I was observing the properties of the printed film.

3.1 Material properties of the ITO

First of all, I have evaluated a commercial ITO composite. The size distribution of ITO composites was analyzed by transmission electron microscopy (TEM) as shown in the Figure 3.1 (a). The ITO composites revealed well-defined shape with 20-30 nm diameters. We measured 100 particles to estimate the size distribution of

those composites. The inset of Fig. 3.1 (a) shows the size distribution of ITO composites. The mean diameter (d_{mean}) was estimated to be 38.5 nm with the standard deviation of 5.8 nm. Also, a few numbers of relatively large particles ($d_{\text{mean}} > 80$ nm) were also observed. However, we thought that the commercial ITO composite can be used for screen printing because we used a screen with a relatively large linewidth (~1mm). Also, Puetz et al reported a successful result of the screen printed ITO layer. They used a mask with 100 μm linewidth and 25~50 nm diameter ITO nanoparticles. [5] We considered that the linewidth to particle size ratio for this experiment is large enough to applicable printing process.

The Fig. 3.1(b) is the X-ray diffraction pattern of the ITO composites and printed ITO layer. The strong diffraction peaks were assigned to (222), (400), (440) and (622) planes of cubic bixbyite ITO (JCPDS 01-089-4198). Although, we have mentioned that the size of ITO grain increased during the debinding process. However, from the XRD result no clear evidence of crystalline phase change was observed because the process temperature was not high enough to induce crystal phase change. Aiempanakit et al have reported that improving crystallinity from 350°C [6]. After annealed at high temperature, the ITO film showed a better crystallinity in terms of the XRD intensity increasing.

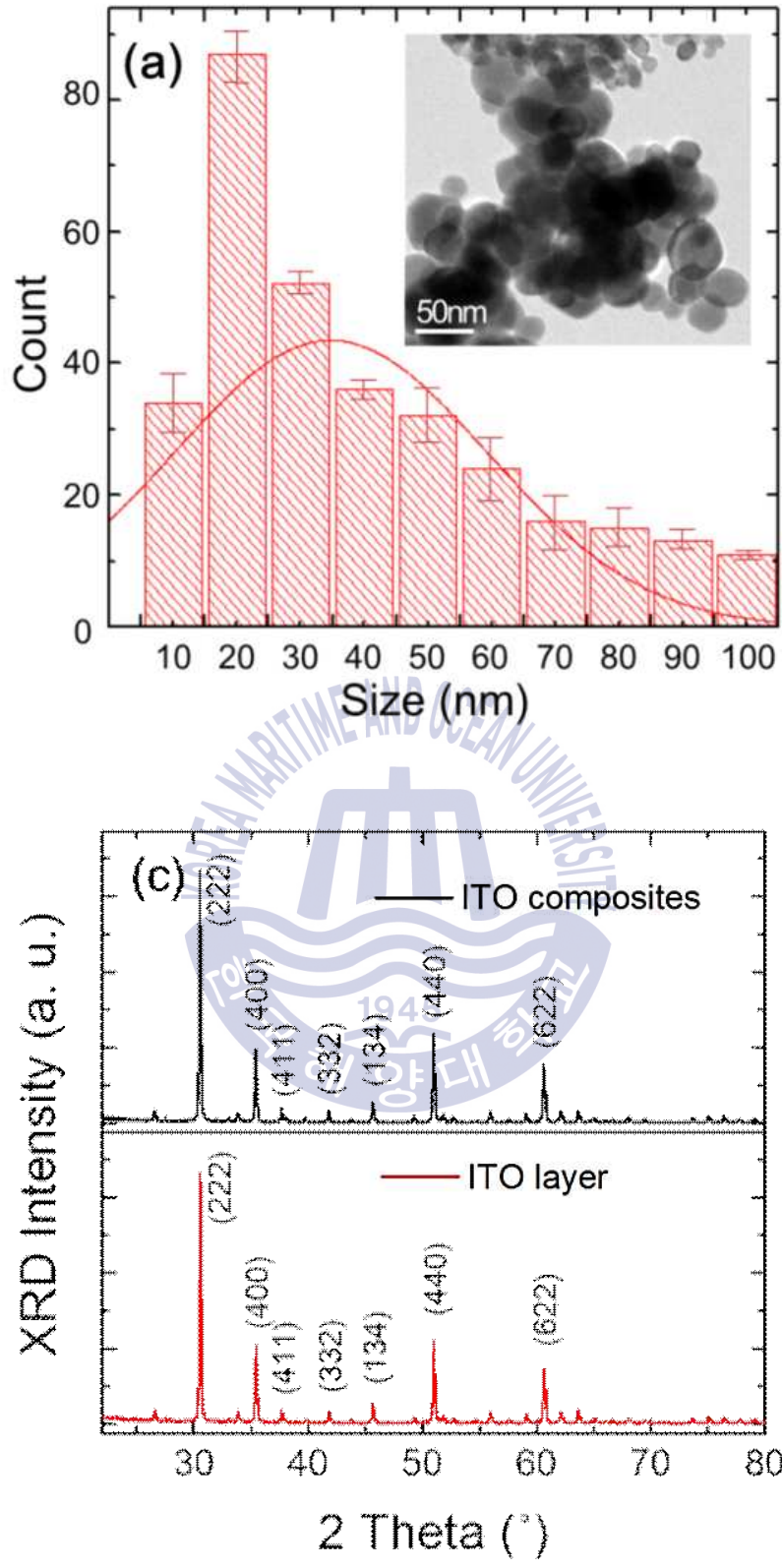


Figure 3.1 (a) Particle size distribution of ITO composites (the insert is the TEM image of it), (b) XRD pattern of ITO composite.

3.2 Optimization of the printed ITO layer manufacturing method

In this section, in order to fabricate a good ITO layer, I observed the changes in the surface energy of the quartz substrate. Due to a change in the substrate surface energy, I was observing the optimization of the layer production

3.2.1 Characteristics of layer patterns on the surface energy of quartz substrate

Table 3.1 is the result of the comparison in order to observe the change of the surface energy of the substrate. It confirmed the change in shape of the print pattern after the substrate cleaning using an organic cleaning and isopropyl alcohol. After that, it was confirmed surface energy value through the contact angle. Isopropyl alcohol was dissolved nonpolar material and serves to remove the oil of the glass. [7, 8]

It was cleaned sequentially with acetone, methanol and DI water in an ultrasonic bath to remove organics and impurities on the surface, where each step took 15 minutes. Other substrate cleaned sequentially with isopropyl alcohol and DI water in an ultrasonic bath to remove impurities on the surface, where each step took 15 minutes too. And then, I was printed on each of the substrates. For the case of these two, I compared the pattern shape and surface energy. The shape of the printing pattern was observed using an optical microscopy, the surface energy is to measure the contact angle measurement.

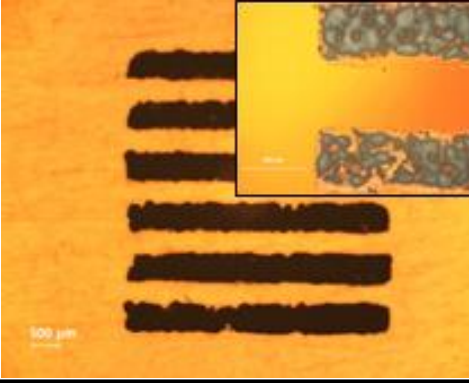
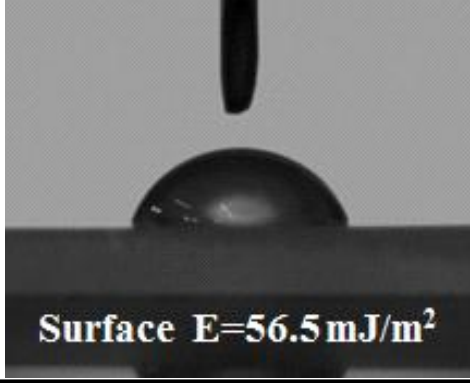
First, the organic cleaning-printed pattern is shaped like partial breakage. The value of the surface energy by organic cleaning is $56.5 \text{ (mJ/m}^2\text{)}$. On the other hand, isopropyl alcohol cleaning-printed pattern is shaped an unbroken. The value of the surface energy by isopropyl alcohol cleaning is $35.8 \text{ (mJ/m}^2\text{)}$.

These results are distinguished from typical thin film growth. In a typical thin film growth, If the surface energy of the substrate is low, island growth tends to proceed. However, In this experiments, It obtained a uniform thin film and precision printing pattern with low substrate surface energy. These results can be explained by leveling as shown Fig. 3.2 [9]. In printing process, In order to pastes is supplied through a screen. In this case, when the surface tension of paste (γ_p) should be

bigger than the surface energy of screen (γ_{scm}), adhesive force is reduced. It is possible to print the surface of the substrate (γ_s). The surface energy of substrates is bigger than the surface tension of pastes, to attractive force is generated. It is possible to form the printing pattern. Therefore, $\gamma_s < \gamma_p < \gamma_{scm}$ is necessary in printing process. However, When the surface energy of the substrate is too big ($\gamma_s > \gamma_p$), it is suggesting that the print pattern can not be formed.



Table 3.1 Optical microscope image of printed ITO layer.

Cleaning procedure	Morphology	Surface energy
Organic solvent		
Isopropyl alcohol		

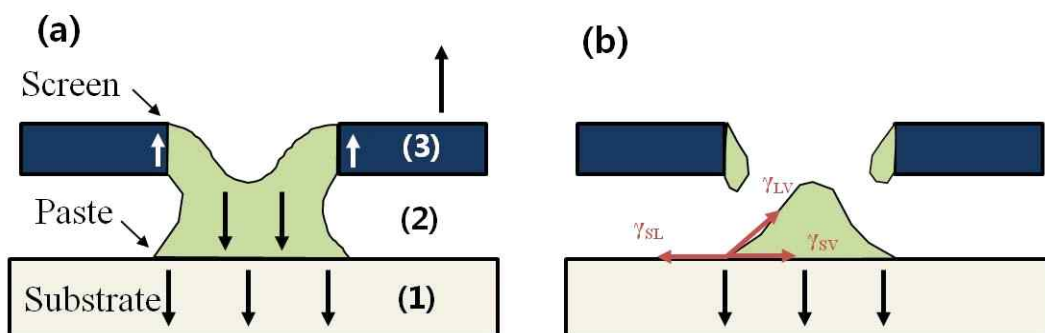


Figure 3.2 Effect of surface tension of paste on screen printability (a) separating (b) leveling.

3.2.2 Print transfer rate characteristics of the ITO layer

Fig. 3.3 is comparing the printed pattern of different viscosity ITO pastes. In order to make a different viscosity, We make a different ratio of ITO pastes. (ratio of ITO powder and the binder). Then, we compared the printed pattern of different viscosity ITO pastes by Optical microscope. It was compared in three main relatively ratio of the ITO powder and organic binder. (ratio of ITO powder and binder; 2:1, 1:1, 1:2) The optimized conditions according to the properties of the paste should be defined by the Transfer rate, %. It can appear as shown in Equation 3.1.

$$Transferrate(Rp) = \frac{W_{print}}{W_{pattern}} (\%) \quad (3.1)$$

W_{print} is the spacing of the printed pattern, $W_{pattern}$ is the pattern interval of the screen mask. Utilizing the measured transfer rate results, Fig. 3.3 (a) is shows the I-V characteristics according to the ratio (ITO: organic binder), 1:1 ratio is the lowest resistance value. As shown in Fig 3.3 (b) ~ (d), the implementation of the pattern of the ITO layer is confirmed to be the best in a ratio of 1:1. Unlike the twice of ITO ratio, the edges of printed pattern are neat, moreover When the binder ratio is twice, the edge of the pattern is widened severely. The above-mentioned results, it was possible to know that it is optimized conditions when the ratio of ITO and binder 1:1.

Electrical characteristics of the printing film, it is determined by the average diameter of particles (crystal grain size) and binding rate of coupling between the particles (porosity) [5]. In this experiment, since the using particles was same, porosity is determined that the magnitude of the electrical resistance. Ethyl cellulose has been known as an insulator [10]. The resistance may be decreased using less binder amounts, but actually 1:1 ratio is the lowest resistance value. The reason is, porosity is minimized in an optimum mixture ratio. So the higher the binding rate of coupling between the particles, which is determined that exhibit low resistance. These considerations can be estimated from Fig. 3.3 (b) ~ (d) shown accuracy.

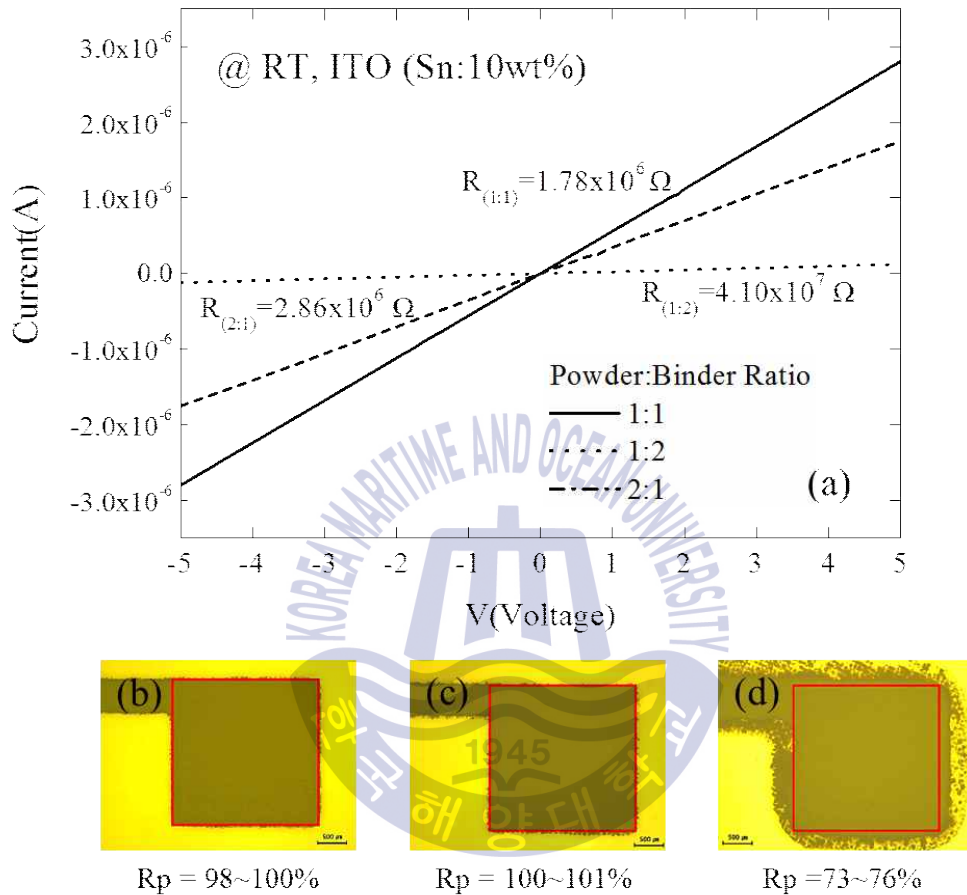


Figure 3.3 The pattern shape dependence of paste ratio in screen printing. (a) Resistance of ITO printed films with various ITO:binder mixing ratio, and the reproducibility of ITO paste with various ITO:binder mixing ratio, (b) 1:1 ratio ($R_p = 98 \sim 100\%$), (b) 1:2 ratio ($R_p = 100 \sim 101\%$), (c) 2:1 ratio ($R_p = 73 \sim 76\%$).

3.3 Properties of the printed ITO layer

Fabricated ITO layer was discussed from the point of view of shape, electrical and optical properties.

3.3.1 Shape characteristics

Using those ITO composites, ITO layers were printed on the quartz substrates. Fig. 3.4 (a) is the FE-SEM images of the surface of printed ITO layer and the inset shows the cross-section of it. From the surface, a porous structure was observed with large grains. Porosity was estimated to be 27~30%. Note that the nominal grain size in the Fig. 3.4 (a) (ranging 100 ~ 200 nm in diameter) is considerably larger than the ITO particles observed from the TEM observation (Fig. 3.1(a)). It indicates that the large ITO grains were formed during the debinding process at low temperature.

The inset of Fig. 3.4 (a) is the cross sectional view of the printed ITO layer. Porous structure with large ITO grains was also observed. The porosity estimated from the cross-sectional image was ~27%, which corresponds well with the porosity obtained from the surface image. The thickness of the layer was found to be $10 \pm 1 \mu\text{m}$. Consequently porous ITO layer was obtained which is suitable for the sensor application.

To monitor the electric signal from the ITO layer, we made contacts at the both ends of the ITO layer using a silver paste. Fig. 3.4 (b) is the photograph of the printed ITO sensor.

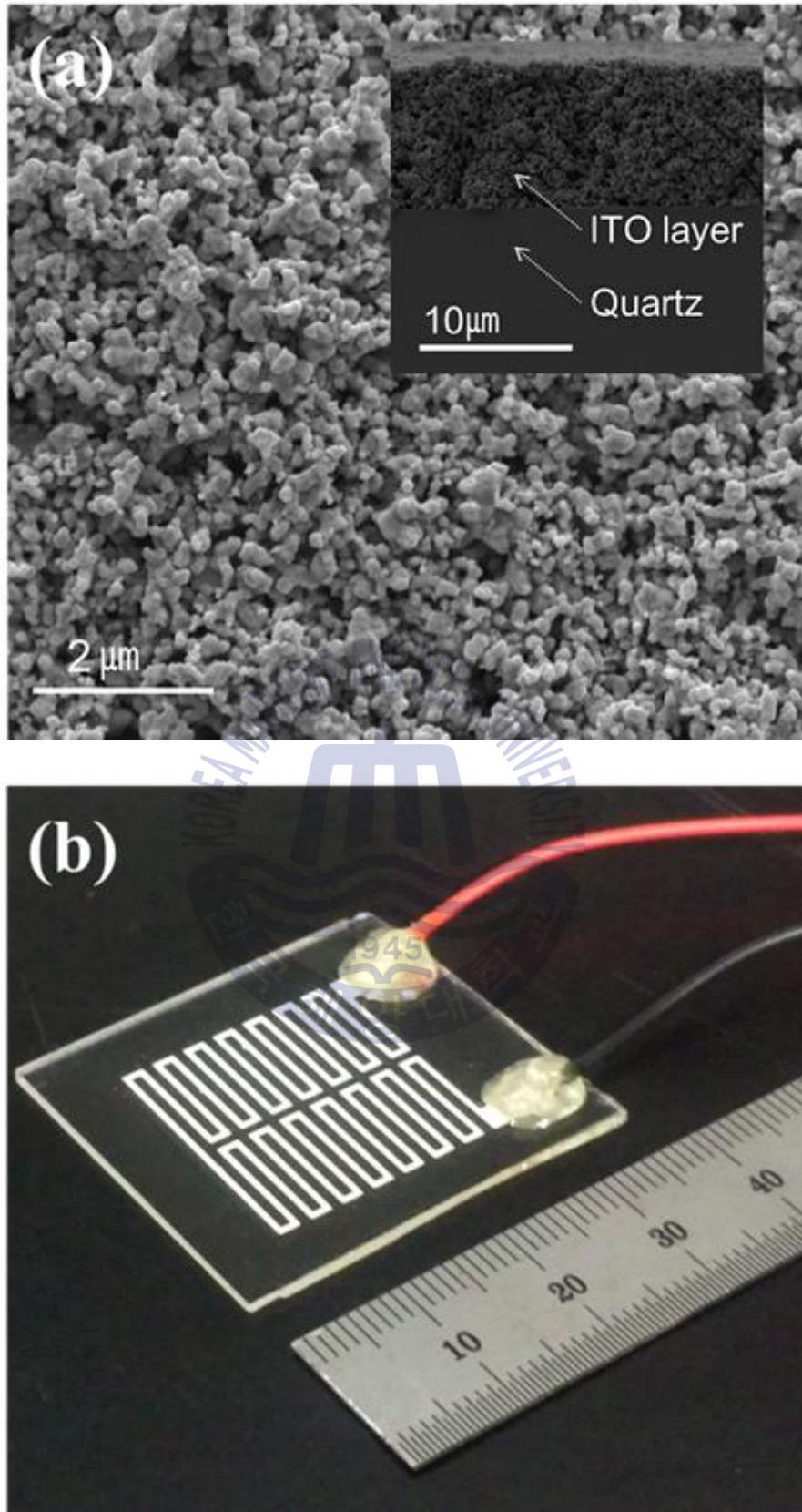


Figure 3.4 (a) FE-SEM images of ITO layer (the inset is the cross section of it), (b) Photograph of the printed ITO layer sensor.

3.3.2 Electrical characteristics

Fig 3.5 is the change in resistance of the ITO thin film is grown by printed ITO layer and the sputtering shown in I-V graph. Thin film ITO grown by sputtering has a specific resistance of $0.050 \Omega \cdot \text{cm}$, printed ITO layer having a high specific resistance of $22.51 \Omega \cdot \text{cm}$. Such changes in electrical properties, we can confirm the measurement results of the Table 3.2. Table 3.2 is a Hall measurement result of the ITO thin film is a printed ITO layer and grown by the sputtering. Printed ITO layer shows low mobility ($6.2 \times 10^{17} \text{cm}^{-3}$) and low carrier concentration ($0.16 \text{cm}^2/\text{VS}$) than the ITO thin film which is grown by sputtering. Change in the electrical characteristics of printed ITO layer, compared with the ITO thin film which is grown by sputtering, indicating the degradation properties. However, when the comparison of electrical characteristics of an existing printed metal oxide thin film, it is increased the resistivity value of 30%. Printed ITO can be judged to have a range of electrical properties that can be applied to the device. [11, 12]



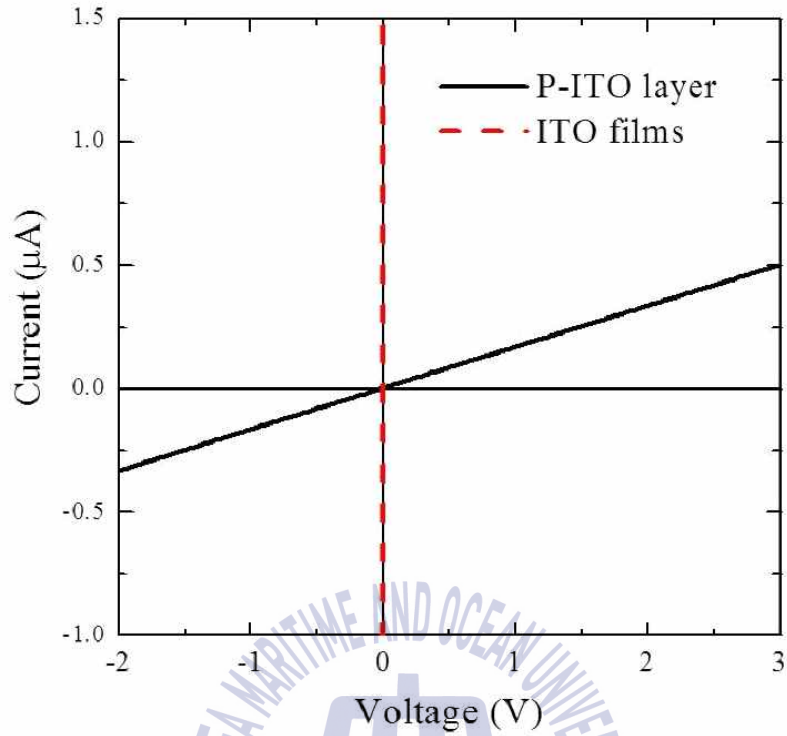


Figure 3.5 I-V characteristics of printed ITO layer and sputtered ITO films.

Table 3.2 Hall measurement of printed ITO layer and sputtered ITO films.

	Resistivity [$\Omega \cdot \text{cm}$]	Carrier concentration [cm^{-3}]	Mobility [cm^2/VS]
Printed ITO	22.51	6.2×10^{17}	0.16
ITO film	0.050	1.31×10^{18}	95

3.3.3 Optical characteristics

Fig 3.6 shows the room temperature PL graph of the printed ITO layer. ITO is an indirect transition semiconductor of wide band gap of 3.8 eV. Emission through the PL measurement should be determined to be caused by deep level due to binding. [13]

In Fig 3.6, it was fitted using a Gaussian equation. As a result, it was possible to confirm the isolated peak of 2.53 eV and 2.9 eV. From the ITO internal defects (oxygen vacancy, indium vacancy, interstitial tin and indium of the defects), Two of the Peak can be assumed that each was caused by the interstitial tin of oxygen vacancy. [14, 15]



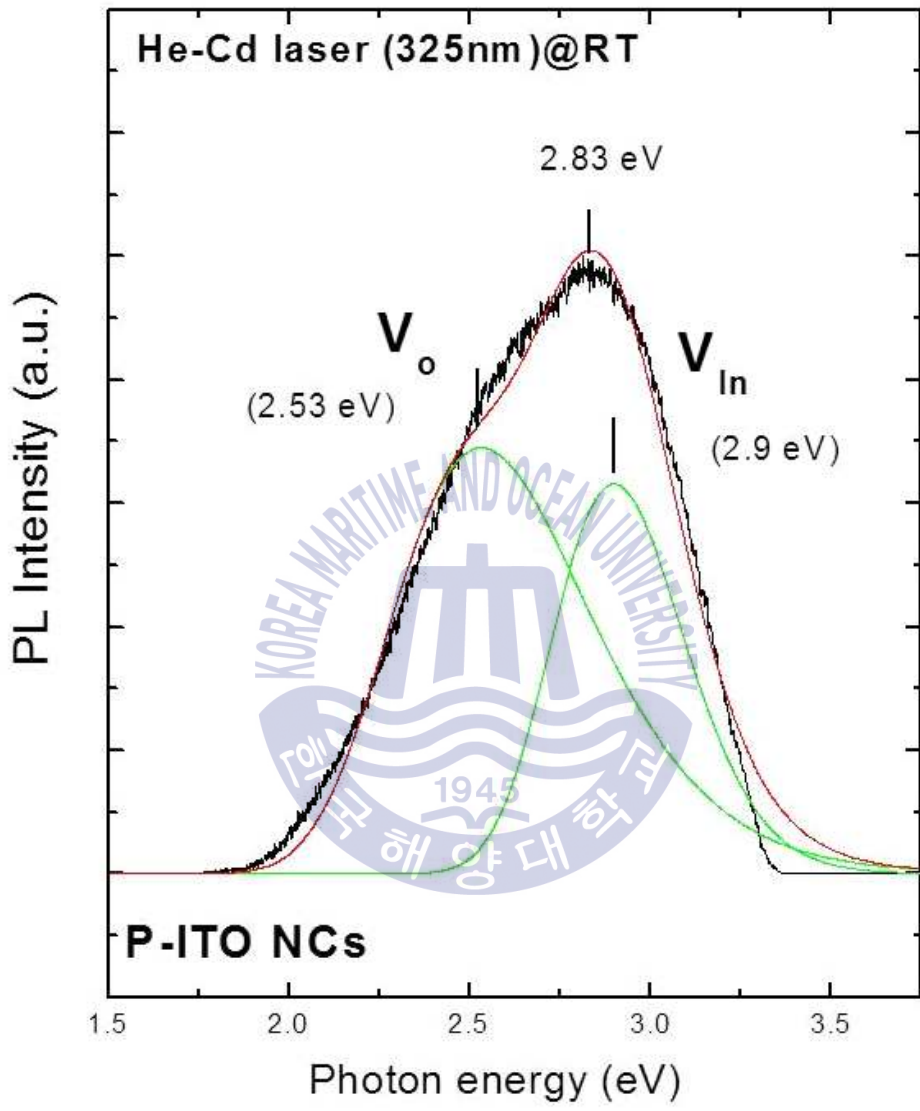


Figure 3.6 PL spectra of printed ITO layer

3.4 Conclusion

In Chapter 3, it was manufactured the ITO layer by screen printing technology in the sensor. Printed ITO layer is optimized for through a transfer rate and substrate surface energy. I have investigated the electrical, shape, optical properties of the fabricated ITO layer before and after. As a result, the printing process was confirmed that does not affect the substance characteristics.



Reference

- [1] Zhang, Tengyuan, et al. "Fabrication of flexible copper-based electronics with high-resolution and high-conductivity on paper via inkjet printing." *Journal of Materials Chemistry C* 2.2 (2014): 286-294.
- [2] Secor, Ethan B., et al. "Gravure Printing of Graphene for Large-area Flexible Electronics." *Advanced materials* 26.26 (2014): 4533-4538.
- [3] Kim, Seung-Hwan, et al. "Effect of Micro Surface Structure on Printed Electronics." *Journal of the Korean Society for Precision Engineering* 27.9 (2010): 20-25.
- [4] Nam, Ki Sang, et al. "Effect of Properties of Conductive Ink on Printability of Electrode Patterning by Gravure Printing Method." *Journal of the Korean Society for Precision Engineering* 30.6 (2013): 573-577.
- [5] Puetz, Joerg, and Michel A. Aegerter. "Direct gravure printing of indium tin oxide nanoparticle patterns on polymer foils." *Thin Solid Films* 516.14 (2008): 4495-4501.
- [6] Aiempanakit, Kamon, Pattana Rakkwamsuk, and D. Grattana. "Characterization of indium tin oxide films after annealing in vacuum." *Kasetsart. J. Nat. Sci* 42 (2008): 351.
- [7] Fang, Mei, et al. "Particle-free inkjet printing of nanostructured porous indium tin oxide thin films." *RSC Advances* 3.42 (2013): 19501-19507.
- [8] Harnett, Elaine M., John Alderman, and Terri Wood. "The surface energy of various biomaterials coated with adhesion molecules used in cell culture." *Colloids and surfaces B: Biointerfaces* 55.1 (2007): 90-97.
- [9] M.Y. Lee, Pukyong National University, 박사학위논문 (2008)
- [10] A. Pasolini, "Zeofrom: The eco-friendly building material of the future?", <http://www.gizmag.com/zeofrom-cellulose-water/28796/>, 2013
- [11] Lai, Hsiang-Yu, Tsung-Han Chen, and Chun-Hua Chen. "Optical and electrical

properties of ink-jet printed indium-tin-oxide nanoparticle films." *Materials Letters* 65.21 (2011): 3336-3339.

[12] Jeong, Jin-A., and Han-Ki Kim. "Characteristics of inkjet-printed nano indium tin oxide particles for transparent conducting electrodes." *Current Applied Physics* 10.4 (2010): e105-e108.

[13] Shaw, J. L., et al. "Deep level photoluminescence spectroscopy of CdTe epitaxial layer surfaces." *Applied physics letters* 56.13 (1990): 1266-1268.

[14] Wu, Ping, et al. "Correlation between photoluminescence and oxygen vacancies in In₂O₃, SnO₂ and ZnO metal oxide nanostructures." *Journal of Physics: Conference Series*. Vol. 188. No. 1. IOP Publishing, 2009.

[15] Kim, H. S., et al. "Synthesis, Structure, Photoluminescence, and Raman Spectrum of Indium Oxide Nanowires." *Acta Physica Polonica A* 119.2 (2011): 143-145.



Chapter 4. HNS sensor based on printed ITO layer

4.1 Introduction

The Hazardous and Noxious Substances (HNS) spill accidents in the ocean have been recognized as a critical problem for marine life, to damage amenities or to interfere with other legitimate uses of the sea. [1] Unlike the oil spills, however, HNS spill issue was not getting spotlight so far. Note that there are two basic ways of HNS detection by using spectroscopic methods and direct chemical reaction on the sensor surface. However, those ways neither provide high spatial resolution and tracking ability, although those issues are essential for minimizing the HNS spill accident damage in the ocean. One possible solution is making a floating sensor network around the dangerous area on the ocean surface. Hence, light-weight and mass-producible sensor is inevitable for developing an advanced HNS prevention system.

We were focused on ammonia (NH_3) in HNS. It is because the ammonia is one of the substances that utilize maritime transport and commonly used to apply many commercial products. [2] Ammonia has caustic, hazardous, colorless and pungent odor characteristics in its concentrated form. [3] In addition, ammonia creates environmental pollution by forming smog and collapse nitrogen cycle system. Hence, ammonia detection in ocean has an importance.

In this Chapter 4, it is to carry out the operation evaluation of the sensor with respect to ammonia, it is intended to describe the sensor mechanism.

4.2 Experiment details

I made a paste for printing that contains the ITO powder (90% In_2O_3 , 10% SnO_2 , # 2731BY) and an organic binder (ethyl cellulose + α -terpineol) with 1:1 weight ratio. We used a quartz (SiO_2) substrate. The size of the substrate is about $35 \times 35 \times 1$ mm³. It was cleaned sequentially with methanol, acetone and DI water in an ultrasonic bath (each step took 15 min) to remove organics and impurities on the surface. ITO powder was printed using a zigzag-pattern mask (thickness: 30 μm , mesh size: 325 inch^{-1}) on a quartz substrate. After printing, the ITO layer was

heated at 200 °C for 1.5 h in order to remove the volatile organic solvent in the printed layer (debinding process). We have optimized the viscosity of the paste in terms of the transfer ratio which means the ratio between the linewidth of original pattern and printed one. To monitor the electric signal from the ITO layer, we made contacts at the both ends of the ITO layer using a silver paste.

We have recorded the resistance of the sensor in the air as a reference signal, and monitored the variation of it by soaking in the seawater and the ammonia hydroxide solutions. We have monitored the temporal variation of resistance in the air and soaked in the solutions. We used four different liquids; seawater, 5% NH₃ in seawater, 10% NH₃ in seawater, and 20% NH₃ in seawater solution. Floating platform is necessary to position the sensor on the liquid surface. The ITO layer is placed just beneath the platform. I-V characteristics were measured under a DC bias of 5V using a Keithley 2400V instrument.

4.3 Sensor properties

To investigate the feasibility of the ITO layer as a HNS sensor, we have monitored the resistance change of the ITO layer in according to the various liquids as shown in the Fig. 4.1. First of all, to find out a reference signal level, the resistance of the ITO layer has been monitored in the air for 100 seconds, and then the ITO layer was soaked in the liquids. The resistance of the ITO layer abruptly dropped, and slowly increased to a certain value from all samples.

Note that, the estimates of resistance change range in 2 ~ 4 orders, also it is correlated with the kind of liquid. The reference signal (initial resistance values in the air) of the ITO layer is as large as $4.0 \pm 0.1 \times 10^9 \Omega$. Then, it dropped to its minimum value by soaking in the liquids. The minimum resistances were respectively $4.9 \times 10^6 \Omega$ (0% NH₃ in seawater solution), $8.4 \times 10^5 \Omega$ (5% NH₃ in seawater solution), $7.7 \times 10^4 \Omega$ (10% NH₃ in seawater solution), and $7.1 \times 10^4 \Omega$ (20% NH₃ in seawater solution). The sensors were kept in the solution without any excitations, however, the resistance increased to a certain values (after 5~15 seconds of stabilizing time), which are also related with the NH₃ concentration of the solution; $3.2 \times 10^7 \Omega$ (0% NH₃ in seawater solution), $1.6 \times 10^6 \Omega$ (5% NH₃ in

seawater solution), $2.0 \times 10^5 \ \Omega$ (10% NH_3 in seawater solution), $1.5 \times 10^5 \ \Omega$ (20% NH_3 in seawater solution), respectively. Figure 1 clearly implies that the printed ITO layer can be used for ammonia hydroxide detection in the seawater, since both initial and saturated resistance values are closely related with the concentration of solution. Here, it should be mentioned that when a large amount of HNS spill out into the ocean, high concentrations of HNS might be not maintained long time, because physical and chemical reactions will dilute it. [4] Consequently, the highest residual HNS concentration could be estimated to be no more than ~10%, because high HNS concentration could not be maintained for long time due to the physical and chemical dilution in the ocean. Therefore, we have evaluated the sensor performance within the estimated range.



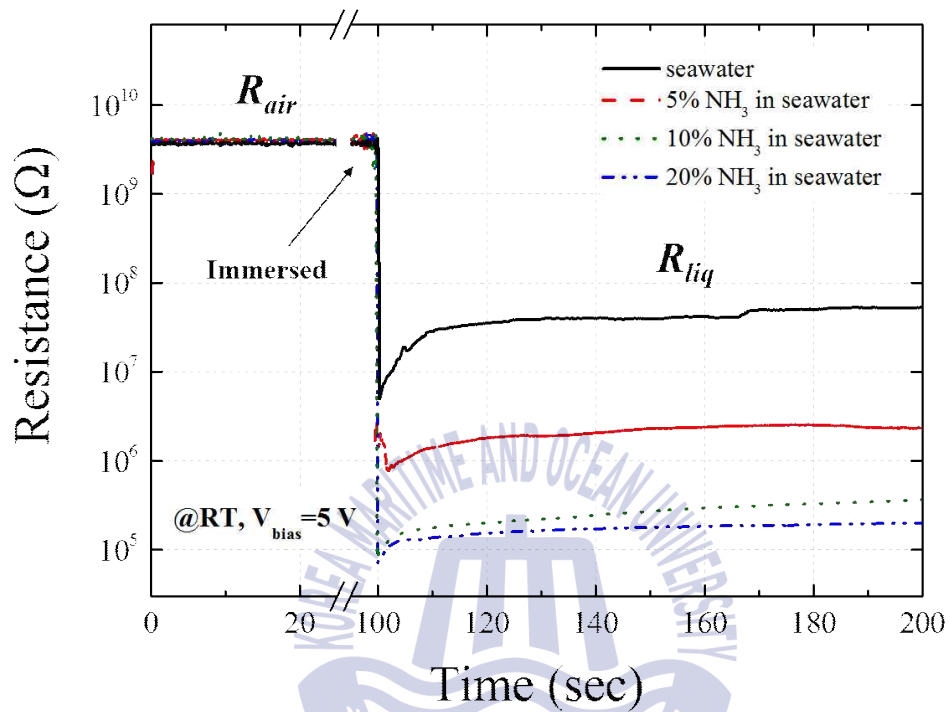
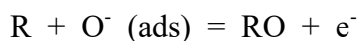


Figure 4.1 Time resolved resistance change of the ITO layers soaked in the various solutions

4.4 Sensor mechanisms

The resistance change of the ITO layer (shown in the Fig. 4.1) can be simply explained by the redox reaction and the electrical double layer (EDL) formation. In generally, redox reactions (oxidation-reduction reactions as shown Fig. 4.2) are simultaneous reactions, meaning they cannot occur without each other. Oxidation means the loss of electrons during the reaction and reduction is classified as the gain of electrons in a reaction. Due to the change of free electron density, the conductivity of material will be changed. Remind that when ITO layer is soaked into the solution, the resistance has dropped. It means that free electron density at the surface has increased by the reduction. On the surface of ITO layer, oxygen is easily adsorbed on ITO surface. When the ITO layer is soaked in an aqueous solution, however, desorption of oxygen from the surface happens as follows (reduction reaction). [5,6]



Where, “R” indicates a reduction agent. It can be not only ammonia but also electrolytes in seawater too. As one can see, however, the resistance change is closely related with the concentration of ammonia. Hence, we considered that dominant reduction agent might be an ammonia in this experiment. As a consequence of this reaction, electrons are liberated, and the carrier concentration of ITO layer increases. Therefore, the resistance of it decreases abruptly as described. It should be noted that one should consider the effect of electrolytes in the seawater also. Thus, the net influence of ammonia itself should be expressed as the difference between the resistance of the NH_3 solutions and that of the seawater. Since the reaction happens in an electrolyte, electronic double layer (EDL) will also be formed near the sensor surface. [7,8] It is well known that the EDL is consisted with two layers; the first layer (stern layer) comprises counter ions adsorbed onto the surface due to chemical interactions and the second layer (diffuse layer) is composed of ions attracted to the surface charge via the Coulomb force, electrically screening the first layer. This second layer is loosely associated with the surface. Formation of EDL will make an equilibrium state near the surface and further resistance change will be hampered as shown in the Fig. 4.3.

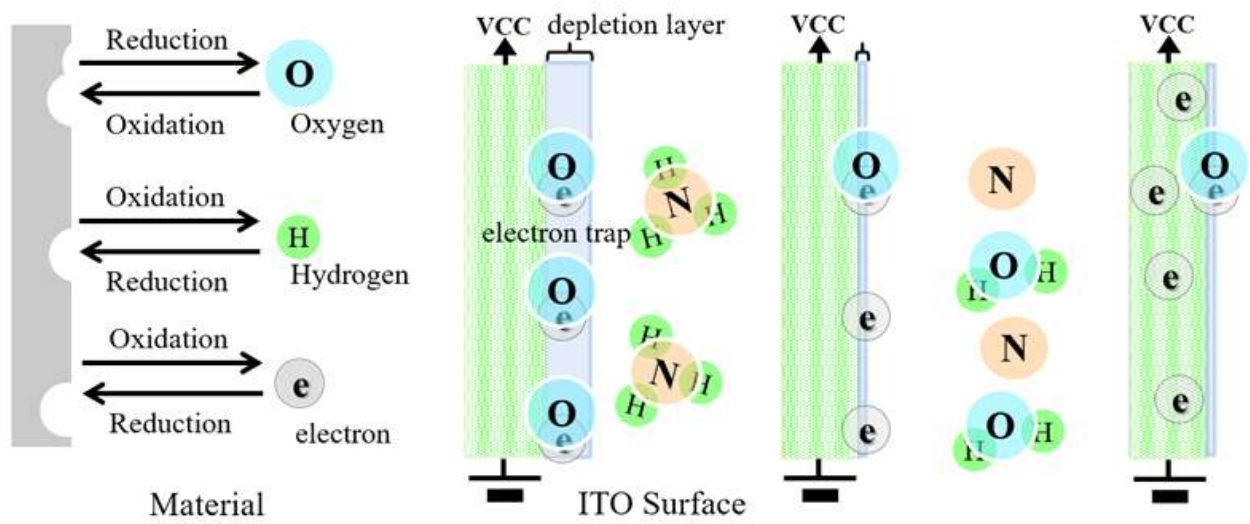


Figure 4.2 Mechanism of reducer agent for ITO layer

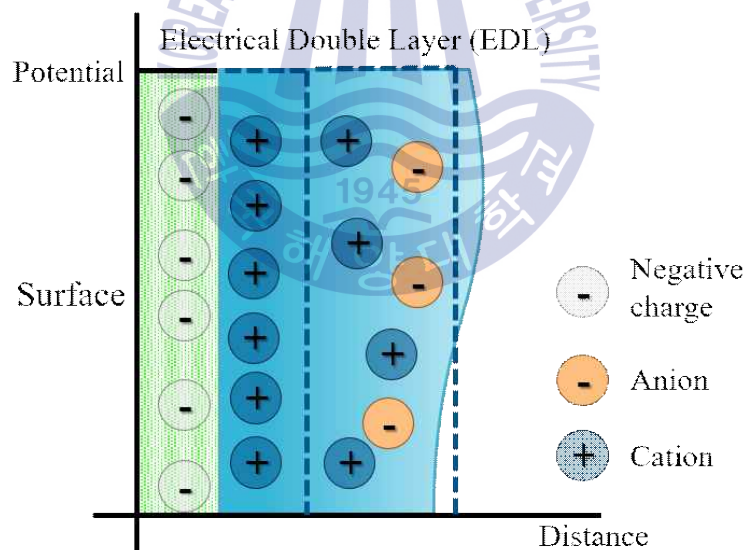


Figure 4.3 Schematic of Electrical Double Layer

4.6 Conclusions

In Chapter 4, it was used a test solution (DI water, Seawater, DI water, seawater, 5%, 10% and 20% ammonia in sea water solutions) to examine the possibility of operating a printed ITO thin film as the room operable sensor. Mechanism of the sensor of sensitivity, I have discussed reducing reaction and EDL model. And we suggest that it is possible to operate at room temperature because our study, it was possible to determine the possibility of hazardous substances sensor applications.



Reference

- [1] International Maritime Organization. Protocol on Preparedness, Response and Co-operation to pollution Incidents by Hazardous and Noxious Substances, 2000 (OPRC-HNS Protocol)
- [2] Are HNS Spills more Dangerous than Oil Spills ? : ITOPF, http://www.itopf.com/fileadmin/data/Documents/Papers/interspill09_hns.pdf (accessed May 2014).
- [3] Toxic FAQ Sheet for Ammonia: Agency for Toxic Substances and Disease Registry, <http://www.atsdr.cdc.gov/tfacts126.pdf> (accessed September 2004)
- [4] Hazardous and Noxious Substances (HNS) Chemical Fate and Effects: ITOPF, <http://www.itopf.com/knowledge-resources/documents-guides/hazardous-and-noxious-substances-hns/chemical-fate-and-effects/> (accessed May 2014).
- [5] Rout, Chandra Sekhar, et al. "Ammonia sensors based on metal oxide nanostructures." *Nanotechnology* 18.20 (2007): 205504.
- [6] Makhija, K. K. "Arabinda Ray, RM Patel, UB Trivedi and HN Kapse Bull." *Mater. Sci.,(Indian Academy of Sciences)* 28 (2005): 9-17.
- [7] Zhang, Li Li, and X. S. Zhao. "Carbon-based materials as supercapacitor electrodes." *Chemical Society Reviews* 38.9 (2009): 2520-2531.
- [8] Bourikas, Kyriakos, et al. "Adsorption of cobalt species on the interface, which is developed between aqueous solution and metal oxides used for the preparation of supported catalysts: a critical review." *Advances in colloid and interface science* 110.3 (2004): 97-120.

Chapter 5. Reliability of the printed ITO layer based sensor

5.1 Introduction

The sensor basically is important to ensure the sensor functions such as the response of the sensor and accuracy of sensors. Furthermore, in order to systematize the sensor, it is considering the purpose, target, location, state/condition and period of the sensor application system. This chapter considered as a whole sensor system along with the function of the sensor. Sensor systems have conditions such as reliability of safe operation, Long life, easy to repair, and economic efficiency on the price. Especially in harsh environments, the bigger the restriction on the conditions described above. So, research of reliability is also necessary.

In the 5 chapter, I was confirmed the reliability of the ITO layer sensor fabricated by screen printing technology. To confirm the reliability, it was tested in various concentrations / temperatures / sensitivity. And the stability of the sensor I was also confirmed. Experiment details

5.2 Experiment details

In this experiment, to prepare a ITO layer using a screen printing method in Section 4.2. To verify the reliability, it was used ammonia in varying concentrations (0~30%). Operation in the temperature interval of the surface of the sea (0~30 °C) it was also confirmed.

In order to confirm the stability of the sensor, we have continuously operated the ITO sensor in the solution for 7 days under 5V bias.

We have examined the robustness of the ITO layer because the seawater is a harsh environment especially for the printed devices. The layers were soaked in the seawater for 24 hours under the external bias (5V) at room temperature.

5.3 Reliability of the sensor

5.3.1 Dynamic characteristics of ITO sensor

Fig. 5.1(a) and 5.1(b) reveal the responses of the printed ITO layer sensor. The sensitivity of the ITO layer is defined as Eq 5.1

$$\text{Sensitivity } (S) = (R_{\text{air}} - R_{\text{liq}}) / R_{\text{liq}} \quad (5.1)$$

Where R_{air} and R_{liq} is the resistance in the air and liquid.

As the NH_3 concentration increasing, sensitivity increases also. Linear response was obtained up to the NH_3 concentration of 15%, however, nonlinearity was observed at higher concentration region. Rout et al have observed a similar phenomenon from a SnO_2 and In_2O_3 based NH_3 gas sensors. [1] They observed nonlinear response from both SnO_2 and In_2O_3 gas sensors. SnO_2 based ones revealed comparably stronger nonlinearity and higher sensitivity as well. They argued that the nonlinear response is caused by higher carrier concentrations in the SnO_2 . Also they mentioned that it is potentially related with the grain size. In our experiment, since we just used one kind of ITO powder, grain size effect might be negligible. Therefore, we temporally attributed the sensitivity saturation to the high intrinsic carrier concentration of ITO. Fig 5.1 (b) shows the sensitivity variation along with the ambient temperature change. Note that, it is quite an important factor for the HNS sensor application, because the sea surface temperature is varying from ~ 0 to 30 °C according to the position on earth, also the sensitivity of a sensor is strongly related with the ambient temperature as well. When the ambient temperature varied from 5 to 35 °C, It implies that temperature compensation should be considered for the practical use of ITO layer.

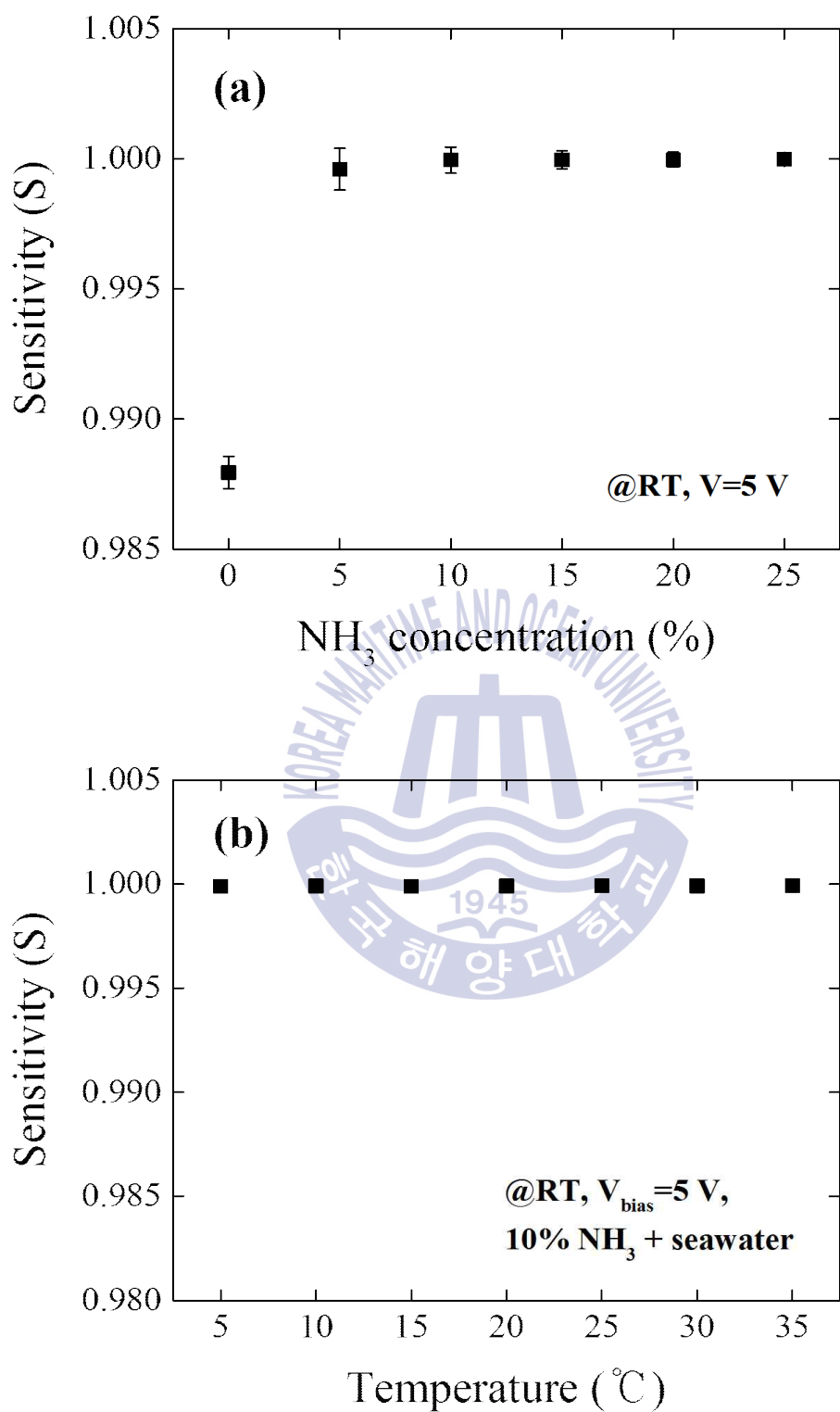


Figure 5.1 Responses of the ITO sensor to (a) different NH_3 concentrations (the inset is the resistance of it), and (b) different temperatures.

5.3.2 Robustness tests of ITO sensor

Stability of the sensor is an important factor especially when you develop a sensor for the utilization in the ocean. Note that, the ZnO sensor was fabricated by the same method, and had the same dimensions with the ITO sensors. Fig. 5.2 shows the SEM images of the (a) as-printed ITO layer, (b) tested ITO layer, (c) as-printed ZnO layer, and (d) tested ZnO layer. As one can see, significant change was not observed from the ITO layer (Fig. 5.2 (a) and (b)), however, dramatic change of surface morphology was observed from the ZnO layer (Fig. 5.2 (c) and (d)). The insets of each picture are corresponding XRD results of the ITO and ZnO layers. The inset of Fig. 5.2 (a) shows the cubic bixbyte phase of as-printed ITO layer with an intense (222) peak at 30.6 degree, and negligible change was obtained from the tested ITO layer as shown in the inset of Fig. 5.2(b). However, clearly different result was obtained from ZnO layers. It's because chloride ions easily can react with ZnO to form ZnCl₂. [2] The inset of Fig. 5.2(c) reveals a typical pattern of hexagonal phase ZnO with an intense (1000) peak at 31.7. While, significant decrease of crystallinity was observed from the tested ZnO layer, which is consistent with the results from SEM observations. Note that, ITO is well known material for various figure of merit. It is considerable that the most important merit is the applicability of chemical etching process in terms of the HNS sensor application.

Further investigation has performed to confirm the stability of the ITO sensor. We have compared both sensitivity and related surface morphology change of ITO- and ZnO-based sensors for 7 days under DC 5V bias. We found that the ZnO-sensor could not endure long-term operation in seawater. Figure 5.3 (a) shows the sensitivity variation of both sensors. Sensitivity of the ZnO-sensor was decreased abruptly after just 2 days operation. However, considerable degradation was not observed from the ITO sensor.

Figures 5.3 (b) and 5.3 (c) show the morphological evolution of both sensors. Dramatic change of surface morphology was observed from the ZnO sensor (Fig. 4(c)). These results indicate the ITO sensor is more suitable for a HNS application in the ocean in terms of chemical stability.

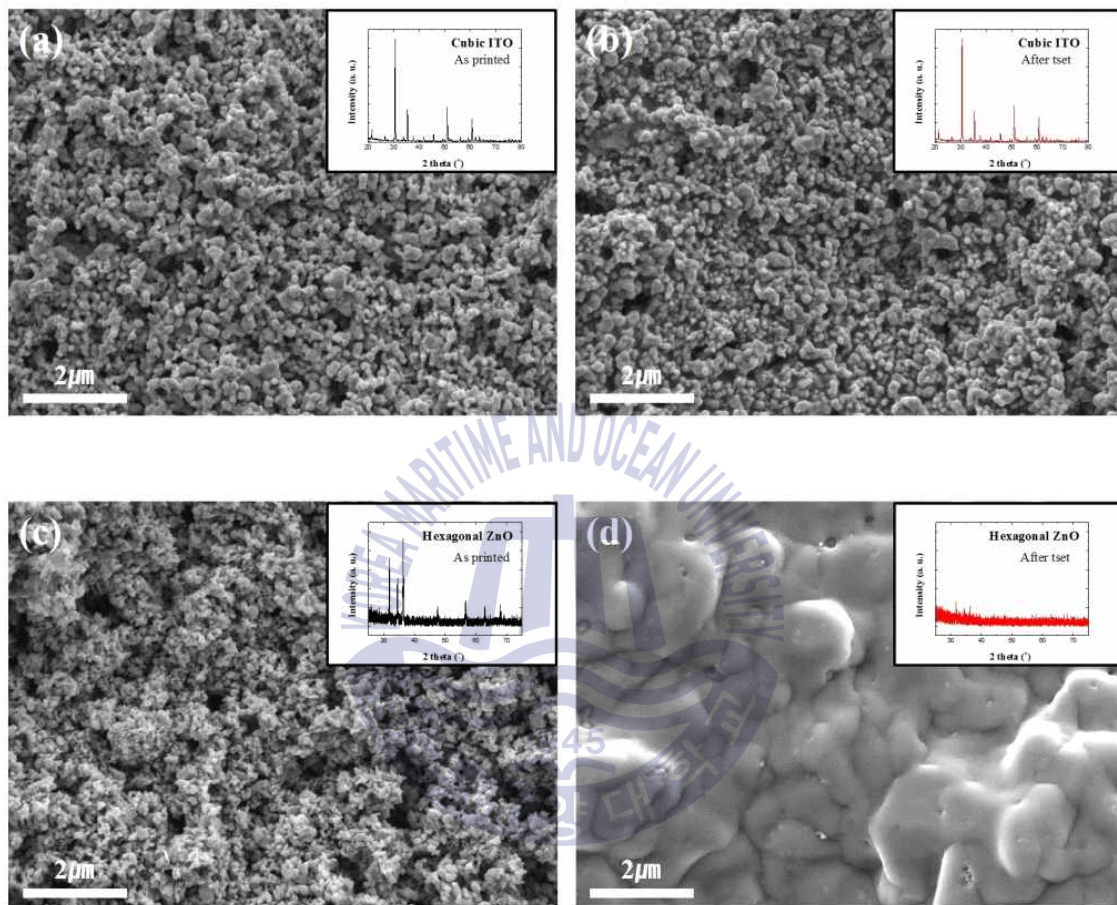
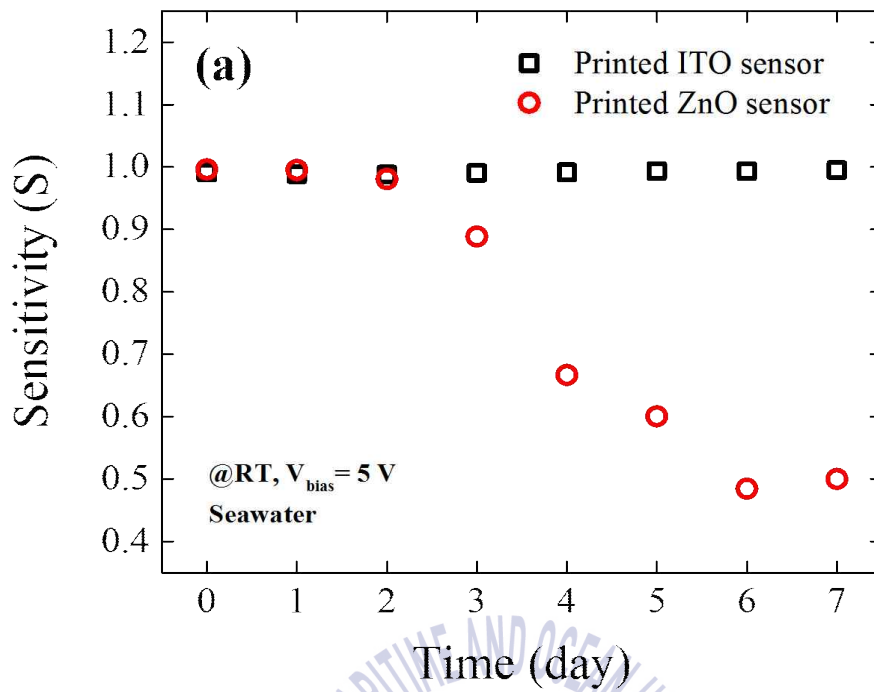
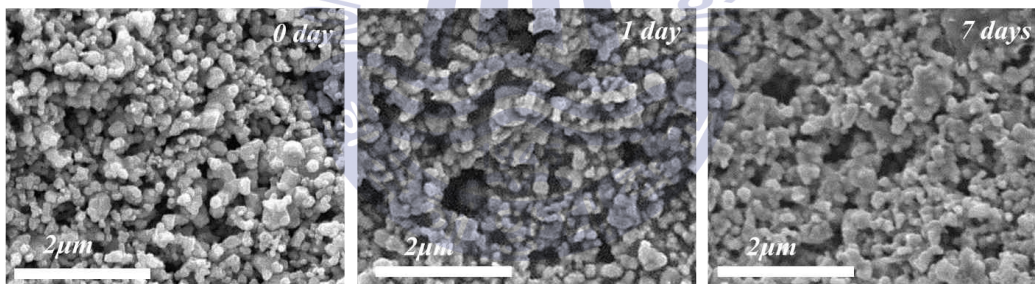


Figure 5.2 FE-SEM images of (a) as-printed ITO layer, (b) tested ITO layer, (c) as-printed ZnO layer, and (d) tested ZnO layer. The insets for each picture are corresponding XRD results



(b) ITO sensor



(c) ZnO sensor

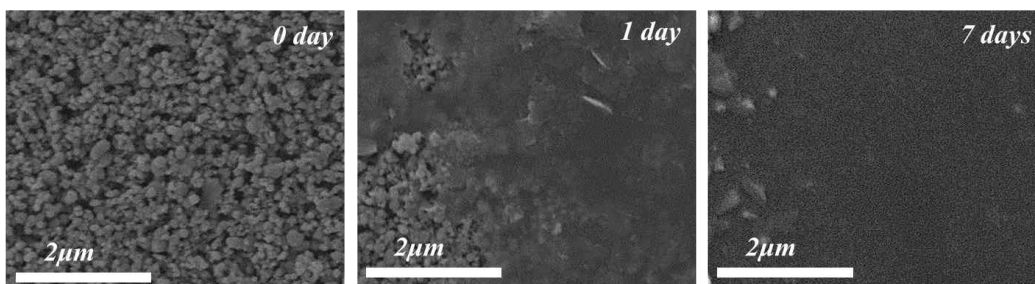


Figure 5.3 (a) The continuous operating test results for the ITO sensors and ZnO sensors during 7 days at room temperature, SEM images of the (b) ITO sensors surface, and (c) ZnO sensors surface during the test.

5.4 Selectivity of ITO sensor

Fig 5.4 shows the change of sensitivity when the ITO sensor contact with the pH solutions. With the increase of pH value, the sensitivity also was found to increase. The response were respectively, 9 (pH 1), 25.18 (pH 3), 56.88 (pH 5), 146.13 (pH 7), 995.00 (pH 9), 4365.47 (pH 11), 25228.98 (pH 13). In this case, the acidic solution is a small increase, the largest growth was observed in the basic solution. As in the aforementioned chapter 4.4, It can be understood as a reduction-oxidation (redox). Oxidation-reduction reactions to occur at the same time, Which initiative reaction will be determined magnitude and direction of resistance. In acid solutions, H^+ is adsorbed on the surface (Dangling bond), bound to the free charge, and it will affect the resistance to increase. On the other hand, In basic solutions, OH^- is adsorbed on the surface. As the pH increases, it has been activated the reduction reaction, concentration of free electrons are rapidly increasing the resistance decreases. These results are shown in Fig 5.4.

Among the material of HNS, substances that pH has been confirmed is a strong alkali and strong acid such as Sulfuric acid (pH 0.3), Hydrochloric acid (pH -1), Phosphoric acid (pH 1.5), Nitric acid (pH 1), Ammonia (pH 11) and Sodium hydroxide (pH 14). Therefore, if a high concentration of HNS are present, it is determined that the sensing area to determine the contamination by neutral value (pH 7).

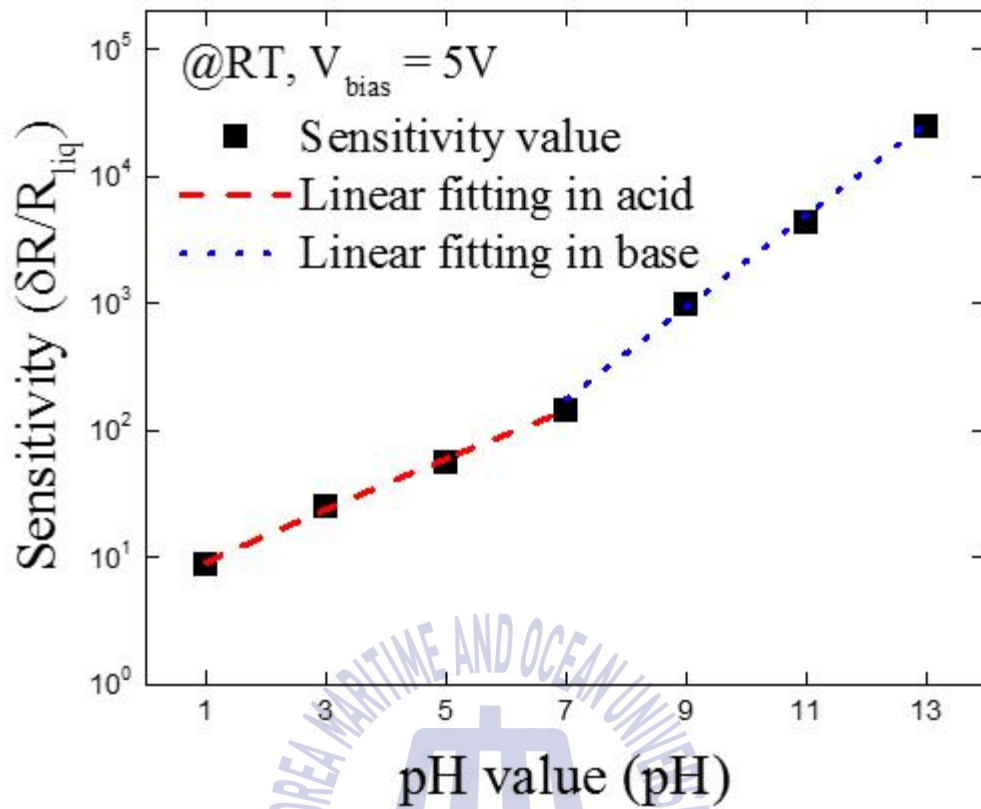


Figure 5.4 Sensitivity change of the ITO layers soaked in the various pH liquids.

5.5 Conclusion

In Chapter 5, I was to reliability and stability performance evaluation as a sensor of the ITO layer film that has been produced by printed printing coat method. It should be mentioned that linear response up to 15% of ammonia hydroxide concentration could be regarded as an enough range in terms of HNS detection in the ocean. it showed results consistent with the previously reported. In the harsh environment of the sea, I was sure that there is a function as a sensor. This ITO layer showed that it is possible to implement as HNS sensor.



Reference

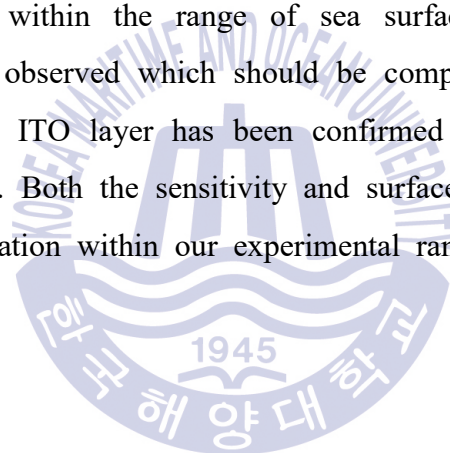
- [1] Rout, Chandra Sekhar, et al. "Ammonia sensors based on metal oxide nanostructures." *Nanotechnology* 18.20 (2007): 205504.
- [2] An, Quanzhang, et al. "Corrosion behavior of ZnO nanosheets on brass substrate in NaCl solutions." *Materials Chemistry and Physics* 115.1 (2009): 439-443.



Chapter 6. Conclusion

In this study, I discussed the possibility of application to hazardous and noxious substances sensor by using the ITO, which is produced by printing coat method.

In order to improve the ITO layer prior to fabricating the sensor, I optimized for the print technology by changing the surface energy and the paste viscosity. This way, Feasibility of printed ITO layer for the HNS detection has been successfully demonstrated. The screen printed ITO layer has a porous structure which is preferred for developing a high sensitivity sensor. Sensor operation was demonstrated by monitoring the time resolved resistance change of the ITO layer. When it is soaked into the solution (sea water + ammonia), resistance varied linearly according to the ammonia hydroxide concentration (<10%). Temperature dependency of sensitivity has evaluated within the range of sea surface temperature (5~30 °C). Considerable change was observed which should be compensated though the driving circuit. Robustness of the ITO layer has been confirmed by a continuous operation (7 days) in the sea water. Both the sensitivity and surface morphology of ITO layer revealed negligible degradation within our experimental range.



R e s u m e

1. 기본정보



성 명	(한글) 이석환	(영문) Lee seokhwan
나이/ 성별	1987년 (만28세) / 男	생년월일 (양) 1987. 08. 04
E-mail	seokhwan-lee@kmou.ac.kr	
전화번호	051-527-7662	휴대폰 010-4230-0804
주 소	(607-825) 부산 동래구 안락 2동 남흥아파트 1 - 1406	

2. 학력사항

년/월/일	학 교 명	학과
2003.03 ~ 2006.02	부산용인고등학교	이과계열
2006.03 ~ 2014.02	한국해양대학교	나노반도체학과
2014.03 ~ 2016.06	한국해양대학교 해양과학기술전문대학원	해양과학기술융합학과

3. 논문 실적

발표 논문명	발표지	발표년도	구분
발광 다이오드(LED)를 이용한 대형 태양전지 패널 평가용 인공 태양광 구성	한국전기전자재료학회	2012	등재지
백색광 LED를 사용한 독서등의 최적 색온도에 따른 사람의 시력 변화 연구	한국전기전자재료학회	2013	등재지
Fabrication of printed ITO sensor for the ammonia hydroxide detection	5th Asia-Pacific Optical Sensors Conference	2015	국외등재지
ITO 인쇄박막을 이용한 원격 감시형 위험유해물질 검출 센서 모듈 제작에 관한 연구	한국마린엔지니어링학회	2016	등재지
전기저항형 금속산화물 센서의 인쇄공정 최적화에 관한 연구	한국전기전자재료학회	2016	등재지

4. 학술대회 발표 실적

발표 명	학술회의 명	발표년도	구분
Fabrication of printed ITO sensor for the hazardous and noxious substances detection in ocean	The 6th International Workshop on Flexible & Printable Electronics	2014	국제
Fabrication of printed ITO sensor for the Ammonia Hydroxide detection	The 5th Asia-Pacific Optical Sensors Conference	2015	국제
Indium-Tin-Oxide 인쇄박막의 제작과 위험유해물질 센서 응용에 관한 연구	제 66회 한국물리학회 부울경 지부 학술대회	2015	국내
Investigation on the sensing mechanism and feasibility of ITO based liquid sensor	The 63th JSAP Spring meeting	2016	국제

5. 국가 연구과제 및 사업 참여

과제 명	지원기관/주관기관	수행기간	비고
ALN를 발광층으로 이용한 200nm 대 심자외 면발광소자의 개발	한국연구재단 / 한국해양대학교	2015 - 2016	
위험유해물질(HNS)사고 관리기술 개발	해수부 - KRISO / 한국해양대학교	2016	

6. 개인능력

어 학	공인 성적	oPic - IL
	영어 쓰기	상
	영어 말하기	중
	기 타	
컴퓨터	OA 능력 (한글/Word/Ms-Office) 전문가 수준	
기 타		

위의 사항이 사실과 다름 없음을 확인함.

2016년 06월 25일 작성자 : 이석환

Acknowledgement

본 논문을 마무리하면서, 많은 사람들의 도움이 있었기에 여기까지 올 수 있었다고 생각합니다. 석사과정 동안 감사했던 마음을 전하고자 합니다.

석사과정 동안, 부족한 저를 대학원 공부까지 할 수 있도록 조언과 지도를 해주신 장지호 교수님께 감사의 마음을 전하고 싶습니다.

전자소재전공 (구 나노반도체) 학과의 이삼녕, 안형수, 양민, 김홍승 교수님께 감사드리며, 학교생활에 도움을 주신 이봉춘 조교님께도 감사의 말씀을 드립니다. 그리고, 논문심사로 도움을 주신 김준영 교수님과 김정창 교수님께도 감사의 말씀을 드립니다. 이 외에도 학문적으로 도움을 주신 정정열 박사님, 이문진박사님과 이정우 박사님께도 감사드립니다.

짧고도 긴, 그리고 많은 일이 있었던 석사과정의 시간이었습니다. 밤을 새면서도 즐거웠고, 논문 발표회를 다니면서도 설렘이었습니다. 물론 그 과정에 있어, 많은 도움을 준 선/후배들께도 감사드립니다. 연구실의 선/후배들로 인간적으로 많이 부족했던 저 자신을 찾았고, 많은 것을 배울 수 있었습니다.

많은 분들께, 감사의 말을 드리며 마지막으로 오랜 기간 동안 뒷바라지를 해주신 부모님과 동생에게도 감사의 마음을 전하고자 합니다.

이상 감사의 말을 줄이며, 다시 한번 더, 저답게 나아겠습니다.

감사합니다.

2016년 6월
이석환 올림